
IN-CONTEXT LANGUAGE LEARNING: ARCHITECTURES AND ALGORITHMS

Ekin Akyürek Bailin Wang Yoon Kim Jacob Andreas
MIT CSAIL
{akyurek, bailinw, yoonkim, jda}@mit.edu

ABSTRACT

Large-scale neural language models (LMs) exhibit a remarkable capacity for *in-context learning* (ICL): they can infer novel functions from datasets provided as input. Most of our current understanding of when and how ICL arises comes from LMs trained on extremely simple learning problems like linear regression and associative recall. There remains a significant gap between these model problems and the “real” ICL exhibited by LMs trained on large text corpora, which involves not just retrieval and function approximation but free-form generation of language and other structured outputs. In this paper, we study ICL through the lens of a new family of model problems we term **in context language learning (ICLL)**. In ICLL, LMs are presented with a set of strings from a formal language, and must generate additional strings from the same language. ICLL is designed to be simple enough to study in small-scale LMs, but complex enough to capture the key features of ICL in large-scale LMs. Here we focus on in-context learning of regular languages generated by random finite automata. We evaluate a diverse set of neural sequence models (including several RNNs, Transformers, and state-space model variants) on regular ICLL tasks, aiming to answer three questions: (1) *Which model classes* are empirically capable of ICLL? (2) *What algorithmic solutions* do successful models implement to perform ICLL? (3) *What architectural changes* can improve ICLL in less performant models? We first show that Transformers significantly outperform neural sequence models with recurrent or convolutional representations on ICLL tasks. Next, we provide evidence that their ability to do so relies on specialized “n-gram heads” (higher-order variants of previously-described “induction heads”) that compute input-conditional next-token distributions. Finally, we show that hard-wiring these heads into recurrent and convolutional models improves performance not just on synthetic ICLL, but natural language modeling—improving the perplexity of 340M-parameter models by up to 1.14 points (6.7%) on the SlimPajama dataset. Our results highlight the usefulness of in-context formal language learning as a tool for understanding ICL in models of natural text.

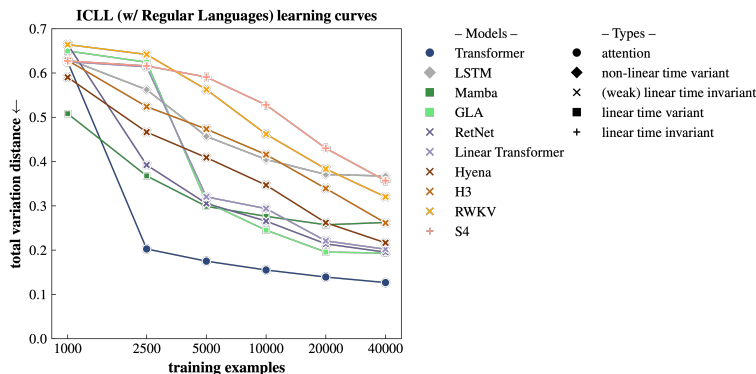


Figure 1: **Transformers effectively learn to perform in-context language learning**, but other model classes (including LSTMs and especially models with time invariant transitions—i.e. efficient convolutional forms) struggle to do so.

1 Introduction

One of the most striking features of modern neural language models is their capacity for **in-context learning (ICL)**—the ability to infer a conditional or unconditional distribution over natural language strings simply by performing next-token prediction following a sequence of examples from the distribution of interest. ICL is a crucial tool for steering large pre-trained language models (LMs), and a growing body of work aims to understand *when* and *how* these LMs perform ICL. Because of the complexity of large-scale LMs trained on natural language text (as well as the lack of public information about many LMs’ training data), almost all work on understanding ICL has instead focused on smaller LMs trained on simple **model problems** like in-context linear regression (Garg et al., 2022), character classification (Chan et al., 2022), and associative recall (Dao et al., 2022). Despite their simplicity, these model problems have played a key role in identifying properties (and limitations) of ICL in current LMs.

However, there remains a significant gap between these model problems and the kinds of capabilities exhibited by LMs trained on large datasets of natural language text. In particular, most model problems require relatively simple forms of learning: computing a fixed function of the entire training set (Akyürek et al., 2022, von Oswald et al., 2023a,b), or retrieving a single example relevant to the current input (Dao et al., 2022). In contrast, natural LMs exhibit richer and much more varied forms of ICL—in some cases producing structured generative models of text or code based on a handful of inputs (Shin and Van Durme, 2022, Drozdov et al., 2022). This requires not just extracting a single summary statistic or example, but instead modeling multiple conditional distributions and re-composing fragments of training examples.

How can we systematically study these more complex forms of ICL? In this paper, we introduce a new family of model ICL problems that we collectively term **in-context language learning (ICLL)**. In ICLL, LMs are prompted with a finite collection of strings from an unknown formal language, and must infer the distribution over strings corresponding to the full language (Figure 2). ICLL exercises essential features of ICL in natural models: it features structured outputs, probabilistic predictions, and compositional reasoning about input data. In this paper, we present a focused study of ICLL in **regular languages**—the class of formal languages generated by finite automata. During ICLL training, each training *example* consists of a sequence of strings from the same language. Different examples feature strings from different languages, so learners must infer language-specific generative models on-the-fly to perform accurate sequence modeling.

We begin by providing general background about neural sequence models, ICL and formal languages in Section 2, then define the ICLL task in Section 3. Next, we explore three questions about in-context language learning in neural sequence models:¹

Q1: Which model classes can learn to perform ICLL accurately? (Section 4)

- We find that Transformers significantly outperform recurrent and convolutional LMs at in-context language learning, even when models perform comparably on other model ICL problems.
- Models with efficient convolutional parameterizations perform especially poorly on ICLL tasks.

Q2: What algorithmic solutions and circuits do successful in-context language learners implement? (Section 5)

- Transformer predictions on ICLL with regular languages are well approximated by smoothed n-gram models.
- Transformers trained for regular ICLL develop “n-gram heads”, higher-order variants of induction heads previously described in LMs (Olsson et al., 2022).
- Compared to other model architectures, Transformers better encode in-context n-gram counts in their hidden representations.

Q3: Can we improve neural models using our understanding of how they perform ICLL? (Section 6)

- Hard-wiring RNNs and convolutional models with n-gram heads improves their performance on ICLL.
- These heads are not just useful for ICLL: when equipped with n-gram heads, neural sequence models of all classes exhibit perplexity improvements of up to 6.7% on natural language modeling tasks.

¹Code and reference implementations are released at https://github.com/berlino/seq_icl

Our results highlights the usefulness of ICLL as a model problem—not only as a tool for research on ICL, but as a source of insight about architectural features that can improve language modeling in the real world. Many aspects of ICLL, even with regular languages, remain to be understood (e.g. learning dynamics and out-of-distribution generalization). Beyond these, ICLL can be extended to even more expressive languages (e.g. context-free or context-sensitive languages), offering a path toward understanding of more complex ICL behaviors in real models. Finally, this paper contributes to a growing body of evidence (Akyürek et al., 2022, von Oswald et al., 2023a) that some instances of ICL are best understood as LMs simulating smaller models (here, n-gram language models) using known parameter estimation and inference algorithms.

2 Background

2.1 Neural sequence modeling

Much of modern natural machine learning for natural language processing is concerned with building general-purpose tools for sequence prediction, in which we wish to place a distribution over strings \mathbf{x} . Very often this is done via a product of conditional distributions over **tokens**:

$$p(\mathbf{x}) = \prod_i p(x_i | \mathbf{x}_{<i}). \quad (1)$$

In practice the distribution $p(x_i | \mathbf{x}_{<i})$ is typically parameterized as a neural network, in which each input token x_i (a symbol, word piece, or word) is assigned an **embedding** e_i , which is used to compute a sequence of **hidden representations** $h_i^{(\ell)}$ (one in each layer ℓ of the network). The last of these is ultimately used to compute the distribution over next tokens. A wide variety of architectural choices are available for computing each $h^{(\ell)}$ from $h^{(\ell-1)}$.

2.1.1 Attentional Networks

Today, the most widely used architecture for neural sequence modeling is the **Transformer** (Vaswani et al., 2017). Hidden representations in Transformers are computed via an attention mechanism: to obtain h_i^ℓ , models compute weighted averages of previous-layer hidden representations $h_{<i}^{(\ell-1)}$ followed by a feed-forward layer. Letting $\mathbf{x} = \mathbf{h}^{(\ell-1)}$ and $\mathbf{h} = \mathbf{h}^{(\ell)}$ for readability, each Transformer layer may be expressed as:

$$\mathbf{h}'_i = \text{softmax}(\mathbf{W}_k \mathbf{x}_{<i} (\mathbf{W}_q \mathbf{x}_i)^\top) \mathbf{W}_v \mathbf{x}_{<i}, \quad (2)$$

$$\mathbf{h} = \text{FFN}(\mathbf{W}_o \mathbf{h}'), \quad (3)$$

where FFN denotes a feed-forward network.

2.1.2 Recurrent and Convolutional Networks

Sequence models other than the attention networks can be characterized as recurrent or/and convolutional:

$$\text{recurrent} \quad \mathbf{h}'_i = \sigma(\mathbf{A} \mathbf{h}'_{i-1} + \mathbf{B} \mathbf{x}_i), \quad (4)$$

$$\text{convolution} \quad \mathbf{h}'_i = \mathbf{l} * \mathbf{x}_{<i}, \quad (5)$$

where \mathbf{A} , \mathbf{B} are recurrence parameters, σ is an activation function, $*$ is a convolution operator and \mathbf{l} is a convolution filter. However, many of these architectures can equivalently be computed with multiple forms, as we review in Appendix A. Hence, we propose a characterization based on *time-invariance* and *linearity*. Time-invariant networks only have parameters that do not depend on input \mathbf{x} , whereas time-variant networks have input-dependent parameters. As a middle ground between them, *weak time-invariant* networks have a mixture of input-dependent and input-independent parameters. In addition, we use *linear* and *non-linear* to characterize recurrent models, based on whether there is non-linear dependencies among hidden states (i.e., whether σ is non-linear).

Linear Time Invariant (LTI) Models Linear and time invariant models usually have both recurrent and convolutional forms. Concretely, their recurrences are linear and the parameters do not change over time, as in $\mathbf{h}'_i = \mathbf{A} \mathbf{h}'_{i-1} + \mathbf{B} \mathbf{x}_i$, where \mathbf{A} , \mathbf{B} are learnable matrices and σ is an identity function and thus omitted. A representative example is the **S4** model (Gu et al., 2022b, along with its many variants, e.g., Gu et al., 2022a, Mehta et al., 2022), which demonstrates competitive performance of such forms on sequence modeling.

Extending the LTI principle, models with weak linear time invariance (WLTI) allow for a time-varying component that can still be captured convolutionally after a suitable transformation. When $\mathbf{h}'_i = \mathbf{A} \mathbf{h}'_{i-1} + \mathbf{B}(\mathbf{x}_i) \mathbf{x}_i$, the \mathbf{B} is not time-invariant anymore, but if it can be written in the form $\mathbf{h}'_i = \mathbf{A} \mathbf{h}'_{i-1} + \mathbf{B} \phi(\mathbf{x}_i)$, it may still be viewed as LTI over the transformed input $\phi(\mathbf{x}_i)$. Next, we list two kinds of WLTI networks from the literature.

Linear Attention as Weak Time-Invariant Networks Linear attention networks such as **Linear Transformers** (Katharopoulos et al., 2020) and **Retentive Networks** (RetNets, Sun et al., 2023) can be represented by recurrent dynamics wherein hidden states are updated through the accumulation of key-value outer products, as in $\mathbf{S}_i = \lambda \mathbf{S}_{i-1} + \mathbf{k}_i^\top \mathbf{v}_i$, where \mathbf{S} denotes 2-D hidden states, and \mathbf{k}, \mathbf{v} denotes key/value vectors (as in attentional networks) respectively. Since the input of the recurrence (i.e. \mathbf{k}, \mathbf{v}) is dependent on \mathbf{x} and λ is fixed, we characterize them as WLTN networks. Moreover, this recurrent perspective reveals that the effective capacity of the hidden states scales quadratically with their dimensionality, offering a potential explanation for the performance of these models.

Weak Linear Time Invariant Convolutional Models The **H3** model (Dao et al., 2022) combines linear attention with a convolutional S4-like layer, resulting in a more complex recurrent form than linear attention with similar input-dependent construction for input (see Appendix A.8). The **RWKV** model (Peng et al., 2023), though not originally presented in a convolutional form, adheres to the LTI principle and can be decomposed into a pair of state space models (SSMs), suggesting a potential for convolutional reformulation (Gu and Dao, 2023; see Appendix A.6). The **Hyena** model (Poli et al., 2023) is a fully convolutional model with data-dependent gating, as in $\mathbf{h}'_i = \phi(\mathbf{x}_i)(\mathbf{l} * \mathbf{x}_{<i})$, where $\phi(\mathbf{x}_i)$ denotes a non-linear mapping of \mathbf{x}_i . We also characterize Hyena as WLTN considering the additional input-dependent mapping $\phi(\mathbf{x}_i)$, compared to vanilla LTI convolutional models.

Linear Time Variant Models Recent state-of-the-art models, **Mamba** (Gu and Dao, 2023) and **GLA Transformer** (Yang et al., 2023), feature fully time-dependent parameterization in both the recurrent and input transformations, as in $\mathbf{h}'_i = \mathbf{A}(\mathbf{x}_i)\mathbf{h}'_{i-1} + \mathbf{B}(\mathbf{x}_i)\mathbf{x}_i$. Their time-variant nature allows for a more flexible and adaptive response to the input sequence, potentially more expressive in terms of sequence modeling. However, these models represent a departure from the LTI framework and pose new challenges for efficient training, as they do not conform to convolutional structures.

Non-Linear Time Variant Models Finally, we also include **LSTMs**, which were the most widely used sequence models in the pre-Transformer era. LSTMs (Hochreiter and Schmidhuber, 1997) feature a complex mapping (σ) based on gating and intermedia cell states in the recurrence, apart from input-dependent parameterizations, as in $\mathbf{h}'_i = \sigma(\mathbf{A}(\mathbf{x}_i)\mathbf{h}'_{i-1} + \mathbf{B}(\mathbf{x}_i)\mathbf{x}_i)$ (see Appendix A.4). Such non-linear time variant models are incompatible with efficient parallel training due to complex dependencies among hidden states. Nevertheless, we include LSTMs to examine their expressivity in comparison to recent sequence models, especially recurrent models.

2.2 In-context learning

One feature that has been observed in all model classes above is their capacity for **in-context learning**. When trained appropriately, sampling from these models given a context of the form:

$$p_{\text{LM}}(\cdot \mid [\mathbf{d}_1, f(\mathbf{d}_1), \bullet, \mathbf{d}_2, f(\mathbf{d}_2), \bullet, \dots, \bullet, \mathbf{d}_n]), \quad (6)$$

yields a high-quality estimate of $f(\mathbf{d}_n)$. Here \bullet is a delimiter token, each \mathbf{d}_i is an input datum, and $f(\mathbf{d}_i)$ is its associated output. In practice, $f(\mathbf{d})$ may be stochastic and compositional, and both inputs and outputs may be structured (e.g. natural language strings with multiple tokens). In addition to this *function-learning* view of ICL, we may understand it more generally as a problem of learning a context-dependent next-token distribution of the same form as Equation (1), for some distribution over strings p_f . Here, sampling from an LM given a context:

$$p_{\text{LM}}(\cdot \mid [\underbrace{x_{1,1}, \dots, x_{1,n}}_{\mathbf{d}_1 \sim p_f}, \bullet, \underbrace{x_{2,1}, \dots, x_{2,n}}_{\mathbf{d}_2 \sim p_f}, \bullet, \dots, \bullet, x_{m,1}, \dots, x_{m,n-1}]), \quad (7)$$

yields an estimate of $x_{m,n}$. By chaining these in-context conditional distributions together, we may sample from p_f .

ICL may be used to turn general-purpose LMs trained into models for specific tasks (like machine translation or sentiment analysis). This pre-training process imposes strong priors on how in-context demonstrations are interpreted (Min et al., 2022)—for example, providing a small number of translated (English, Spanish) sentence pairs in context will induce a pre-trained LM to perform English–Spanish translation, even though the in-context examples do not fully specify the translation process. But in practice models also seem to be capable of some forms of “real learning” in context, inferring functions or distributions within a continuous or combinatorial hypothesis class rather than a fixed set of pre-trained skills (Wei et al., 2023).

While some work on understanding ICL has studied LMs trained on natural text (Olsson et al., 2022, Dai et al., 2023), most interpretability-oriented research has instead studied LMs trained to solve model problems such as linear regression, (Akyürek et al., 2022, von Oswald et al., 2023a), associative recall (Dao et al., 2022) or few-shot classification (Chan et al., 2022). Work in this family studies ICL from several perspectives: as task identification (Xie et al., 2022, Min et al., 2022), string manipulation (Olsson et al., 2022), or a form of learned “mesa-optimization” within a trained LM

(Akyürek et al., 2022, von Oswald et al., 2023a, Dai et al., 2023). But important aspects of ICL in natural models, including stochasticity, structured outputs, are not captured by these model problems, a limitation we aim to address in this paper.

2.3 Formal Languages

We study ICL in the context of a new family of model problems involving formal language learning. In these problems, models condition not on a sequence of (input, output) pairs, but instead on a collection of strings sampled from a randomly generated language. Related language-learning problems were also studied by Xie et al. (2022) and Hahn and Goyal (2023); here we study models’ ability to learn *new* languages rather than recognizing languages from a fixed set seen during training. Below we briefly discuss key concepts useful for defining the ICLL task.

Languages, Strings, and Automata In the context of formal language theory, a **language** L is defined as a set of strings over a finite alphabet Σ . A **probabilistic language** additionally defines an (optionally normalized) distribution $P(x)$ over the strings $x \in L$. An **automaton** is an abstract machine that defines a procedure for testing membership in some language, or generating strings from that language.

Our experiments focus on **regular languages**. These are standardly defined as the set of languages recognized by **deterministic finite automata** (DFAs). A DFA, in turn, is defined by an **alphabet** Σ , a set of **states** \mathcal{S} , an **initial state** $S_0 \in \mathcal{S}$, a subset of **accepting states** $\mathcal{S}_a \subseteq \mathcal{S}$, and a state **transition function** $T : \mathcal{S} \times \Sigma \rightarrow \mathcal{S}$. To determine whether a DFA accepts some string $x = x_1x_2x_3 \dots x_n$, we begin in S_0 , set $S_i = T(S_{i-1}, x_i)$, and finally test if $S_n \in \mathcal{S}_a$.

To extend this definition probabilistic languages, we may generalize DFAs to probabilistic finite automata (PFAs) by redefining the transition function as distribution $T : \mathcal{S} \times \Sigma \times \mathcal{S} \rightarrow [0, 1]$, the initial states as distribution $I : \mathcal{S} \rightarrow [0, 1]$, and the accepting states as distribution $A : \mathcal{S} \rightarrow [0, 1]$. These new distributions satisfy the constraints: $\sum_S A(S) = 1$, $\sum_S I(S) = 1$ and $F(S) + \sum_{x, S'} T(S, x, S') = 1 \quad \forall S$. Under mild conditions $p_{\text{PFA}}(x) = \sum_{S_0, \dots, S_n} \prod_{i=1}^n I(S_0)T(S_{i-1}, x_i, S_i)A(S_n)$ is a proper distribution, where the sum is over all possible state sequences that lead to x .

In this work, we will use simple PFAs with a single initial state, and without any terminal states (sometimes referred to as NFPAs). Then, we can assign probabilities $p_{\text{PFA}}(x) = \sum_{s_0, \dots, s_n} \prod_{i=1}^n T(s_{i-1}, x_i, s_i)$, where the sum is over all possible state sequences starting from the start state that lead to x . It can be proven that this is a proper distribution for each sequence length, with the additional convenient property that it can be equivalently represented with a hidden Markov model²

Formal languages and deep networks A large body of previous work has used formal languages to probe the limits of neural sequence models (Elman, 1990, Gers and Schmidhuber, 2001, Bhattamishra et al., 2020, Suzgun et al., 2019, Hewitt et al., 2020, Finlayson et al., 2022). One line of research has aimed to understand the theoretical expressive power of neural these models. Notably, Merrill (2019) prove that LSTMs with bounded precision can recognize counter languages more complex than regular languages, whereas simple RNNs can only recognize regular languages. Merrill and Sabharwal (2023) show that bounded precision Transformers cannot recognize important classes of formal languages, including some regular languages. Somewhat surprisingly, in light of these theoretical results, our experiments will show that Transformers models outperform recurrent models at learning some regular languages in context, even when they are formally incapable of recognizing even single regular languages in general.

In contrast to this past work, the present study focuses not on whether sequence models can be trained to generate or recognize strings in a *fixed* formal language, but instead whether they can be “meta-trained” to adapt on the fly to new languages provided in context. Closest to this goal, the “associative recall” task studied by Dao et al. (2022), Arora et al. (2023) may also be viewed as a special case of in-context language learning for an extremely restricted sub-class of regular languages; we compare the behavior of models on this task and general ICLL in Section 4. Bhattamishra et al. (2023) study the in-context learning of PARITY and CNF, which may also be cast as formal language learning problems.

3 REGBENCH: A Benchmark Dataset for In-Context Language Learning

What does it mean to *learn* a formal language of the kind described in Section 2? Classical formal language theory has focused “identifiability in the limit”—whether learning algorithms, given access to a potentially unbounded number of strings from a language of interest, can eventually pinpoint that language (Gold, 1967). To understand the behavior

²Please refer to Dupont et al. (2005) for more discussion of the relationship between NFPAs and their equivalence to HMMs.

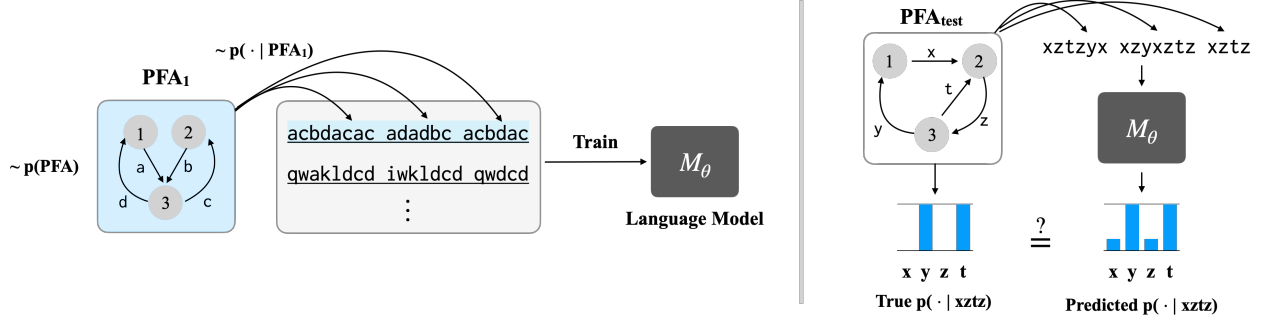


Figure 2: **ICLL Benchmark:** We randomly generate probabilistic finite automata (PFAs) with uniform transition probabilities, and then generate problem instances that include multiple samples from each PFA. We train and evaluate models on disjoint PFAs for in-context language learning.

of current LMs, however, we require both datasets and evaluation metrics more closely aligned with the language modeling task. We thus focus on evaluating LMs’ ability to learn a *distribution* over strings, sampled from a *distribution* over probabilistic languages.

To do so, we introduce a new dataset called **REGBENCH**. REGBENCH consists of a set of **problem instances** $d^{(i)}$, each comprising a sequence of **examples** $[d_1^{(i)}, \cdot, d_2^{(i)}, \cdot, \dots, \cdot, d_n^{(i)}]$, where each example in a problem instance is drawn from the same probabilistic language $L^{(i)}$. To describe how REGBENCH is constructed, we must thus specify (1) how languages are sampled, (2) how strings are sampled from these languages, and (3) how learners are evaluated.

3.1 Sampling stochastic languages

We consider probabilistic languages defined by probabilistic finite automata constructed as follows:

1. Sample a number of states n uniformly from the interval $(n_{\min} = 4, n_{\max} = 12)$. Given this value, define a set of automaton states $\mathcal{S} = \{S_1, \dots, S_n\} \cup \{S_0\}$. Define the set of accepting states $\mathcal{S}_a = \{S_1, \dots, S_n\}$ (excluding S_0).
2. Sample an alphabet size c uniformly from the interval $(c_{\min} = 4, c_{\max} = 18)$. Sample a language-specific alphabet V , containing c symbols, uniformly (without replacement) from a shared symbol set \mathcal{V} (with $|\mathcal{V}| = c_{\max}$).
3. For each S_i , choose a number of outgoing edges m_i uniformly from $(m_{\min} = 1, m_{\max} = 4)$. Then, construct a set of edges (S_i, x_j, S_j) , where all x_j are sampled uniformly without replacement from V , and all S_j are sampled uniformly without replacement from $\{S_1, \dots, S_n\} \setminus S_i$. For every symbol x' not sampled in this step, construct an edge (S_i, x', S_0) . Together, these edges determine the transition distribution for a (non-probabilistic) DFA A .³
4. Construct a new DFA A' by minimizing A (Hopcroft, 1971).
5. Finally, turn A' into a probabilistic automaton without final states by defining each $T(S_i, x_j, S_j) = 1/m_j$ for edges generated above (excluding edges into S_0), and $T(S_i, x', S') = 0$ for all other x', S' .

This procedure may be run repeatedly to obtain a collection of PFAs A' , each with corresponding DFA A , and associated with a stochastic language L .

3.2 Sampling strings

Given a PFA A , sampling from the associated language is straightforward: **(1)** Sample a sequence length uniform between $n_{\min} = 1$ and $n_{\max} = 50$. **(2)** Initialize the sampling procedure with S_0 . **(3)** For each $i \in 1 \dots n$, sample $(x_{i+1}, S_{i+1}) \sim T(S_i, \cdot, \cdot)$. **(4)** Return $x_1 \dots x_n$.

³This particular choice of transition function ensures that each accepted input corresponds to a unique state sequence. This makes it possible to calculate conditional next token probabilities without needing to marginalize over state sequences

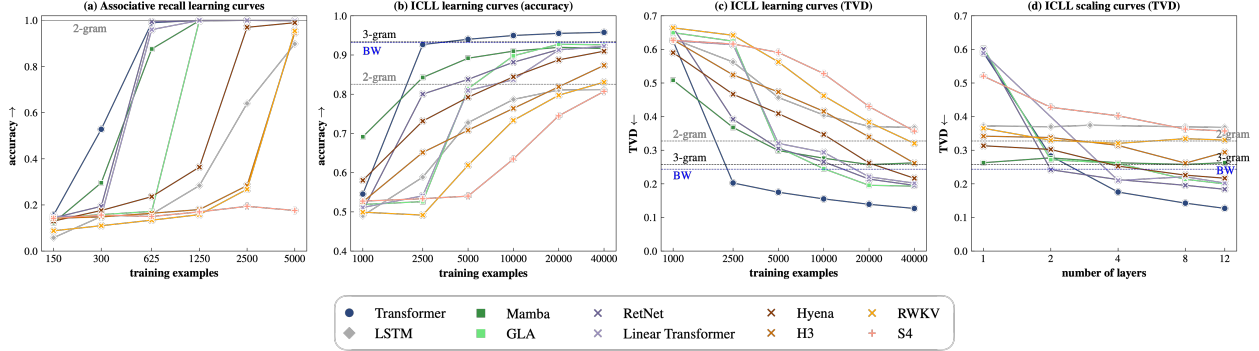


Figure 3: **REGBENCH results:** We propose REGBENCH by extending the previous synthetic benchmarks of in-context learning to in-context language learning with regular languages. REGBENCH (b, c) yields greater contrast between models comparing to associative recall (a), and enables probabilistical evaluation (c). We find that Transformers are significantly more data efficient recent neural sequence model on in-context learning of regular languages or fine state machines. The Transformer model also adhere a monotonichally increasing scaling curves w.r.t number of layers (d).

3.3 Dataset

Using these two sampling procedures, we construct REGBENCH as follows: **(1)** Sample a collection of $N_{\text{train}} + N_{\text{test}}$ distinct automata $A^{(i)}$ using the procedure in Section 3.1. **(2)** From each automaton, sample $n = 10$ to 20 strings $d_j^{(i)}$ with $l = 1$ to 50 symbols each (making the average length of a problem instance $\approx L = 382$). **(3)** Construct problem instances $d^{(i)} = [d_1^{(i)}, \cdot, d_2^{(i)}, \cdot, \dots, \cdot, d_n^{(i)}]$. **(4)** Finally, divide this collection of instances into training and test sets.

As described below, we use this dataset to evaluate the performance of a variety of neural sequence models on ICLL tasks, while comparing it to other diagnostic tests of ICL.

4 Which Model Classes Learn to Perform ICLL Efficiently?

In this section, we use REGBENCH to analyze the behavior of neural sequence models on ICLL tasks. These experiments aim to clarify the relationship between REGBENCH and related existing evaluations of ICL; and most importantly, to determine whether there are meaningful differences between different neural sequence models in their ability to perform ICLL.

4.1 Setup

We train models on the REGBENCH dataset to maximize the likelihood:

$$\mathcal{L}(\theta) = \sum_{d \in \mathcal{D}^{\text{train}}} \log p_{\theta}(x_i | x_{<i}). \quad (8)$$

For comparison, we also train models on the associative recall (AR) task introduced by Poli et al. (2023), using a vocabulary size of $\mathcal{V} = 40$ (based on Poli et al., 2023’s “hard” setting) and an input sequence length of $L = 382$ (which matches REGBENCH’s average sequence length). As with REGBENCH, we use a test set of size 500. For both datasets, we use training subsets of sizes from 150 examples to 40000 examples to evaluate scaling behavior of models.

4.2 Neural Sequence Models

We evaluate 10 neural sequence models: Transformers (Vaswani et al., 2017, Touvron et al., 2023); two Transformer variants with linear attention (RetNet, Sun et al., 2023 and Linear Transformer, Katharopoulos et al., 2020); four recurrent models (LSTM, Hochreiter and Schmidhuber, 1997, RWKV, Peng et al., 2023, GLA, Yang et al., 2023, and Mamba, Gu and Dao, 2023); and three models with convolutional representations (S4, Gu et al., 2022b, H3, Dao et al., 2022, and Hyena, Poli et al., 2023).

4.3 Baseline Learning Algorithms

To contextualize the performance of these neural models, we also compare to two classical procedures for generative sequence modeling. Given the procedure for sampling languages described in Section 3, the bayes optimal predictor has the form:

$$p(x_i | x_{<i}) = \sum_L p(x_i | L)p(L | x_{<i}) \propto \sum_L p(x_i | L)p(x_{<i} | L)p(L), \quad (9)$$

where $p(L)$ is the prior that a given language is produced by the sampling process, and $p(x | L)$ is the probability of an example under L . Unlike model problems like linear regression (Garg et al., 2022, Akyürek et al., 2022), there are no general algorithms known for computing this distribution efficiently. However, simple approaches based on maximum likelihood estimation often perform well. Here we evaluate two:

- **In-context n-gram models:** The simplest baselines we consider are **n-gram** models, which consider a fixed-sized context window of $n - 1$ symbols, locate all matching windows within the problem instance, and simply count the number of occurrences of each possible next token across those matches. Our experiments use a variant with backoff (Chen and Goodman, 1996)—see Appendix C.1 for details.
- **In-context DFAs:** In addition, we compare to a baseline that attempts to explicitly infer the probabilistic automaton that generated the context using the **Baum–Welch (BW)** algorithm (Rabiner, 1989). Given a collection of strings generated by a PFA (or hidden Markov model), this procedure performs maximum likelihood estimation of the transition distribution via Expectation–Maximization (Dempster et al., 1977), then performs inference on given context string to perform next-token prediction—see Appendix C.2 for details.

Note that both of these baselines use only the information available *within* an individual problem instance; unlike the learned models, they cannot pool information about the language-generating process across examples.

4.4 Metrics

We evaluate models using two quantities. The first is a greedy-decoding **accuracy** metric that measures whether each next token predicted by the model is valid under the current regular language:

$$\text{accuracy}(p_\theta, L_i) = \frac{1}{\text{NT}} \sum_{\mathbf{d}_{<j}^{(i)}} \sum_j [\mathbf{1} [\text{argmax}_x p_\theta(x | \mathbf{d}_{<j}^{(i)}) \in \{x' : L_i(x' | \mathbf{d}_{<j}^{(i)}) > 0\}]], \quad (10)$$

where NT is number of total symbols in the test set and $L(x | \mathbf{d}_{<j}^{(i)})$ is the probability of generating x' following the context $\mathbf{d}_{<j}^{(i)}$ in the language L , where this context consists of j tokens comprising of zero or more full examples \mathbf{d} followed by a partial example. To provide a finer-grained picture of how well learners have captured the probabilistic aspect of ICLL, we additionally compute **total variation distance** between each predicted next-token distribution and the distribution allowed under a given language:

$$\text{tvd}(p_\theta, p_{\text{pa}}) = \frac{1}{\text{NT}} \sum_{\mathbf{d}^{(i)}} \sum_j \left[\frac{1}{2} \sum_x |p_\theta(x | \mathbf{d}_{<j}^{(i)}) - L(x | \mathbf{d}_{<j}^{(i)})| \right]. \quad (11)$$

4.5 Results

Evaluation results are shown in Figure 3.

ICLL on REGBENCH shows clear differences across neural sequence models On REGBENCH (Figure 3(b, c)), we find that Transformer models significantly outperform models in all other classes, across both evaluation metrics and a range of training set sizes. Indeed, most non-Transformer models underperform simple n-gram and Baum–Welch baselines, except in the very large data regime.

In contrast, models are less clearly differentiated by the associative recall task (Figure 3a). Here we observe that all neural models except S4 learn to perform this task with 5000 examples, a training setting used in previous work (Dao et al., 2022, Poli et al., 2023). However, even on this benchmark results are somewhat nuanced—in low data regimes, convolutional models (Hyena, H3, S4), LSTM and RWKV perform comparatively poorly.⁴

⁴In concurrent work, Arora et al. (2023) find that increasing vocabulary size above 1k and querying models with multiple key–value pairs also creates greater separation between models.

Deep models are required for ICL, but many models do not benefit from increasing depth In Figure 3, we find that no architecture achieves non-trivial performance on ICLL with only a single layer. Transformer models monotonically improve their accuracy as the number of layers increases; other models start to overfit to the training set with increasing depth, and do not improve their performance on the test set.

5 What Algorithmic Solutions do In-Context Language Learners Implement?

The previous experiments show that Transformers significantly outperform other neural sequence models at regular ICLL. Can we understand *why* these differences occur? In this section, we analyze the behavior of Transformers trained for ICLL tasks identify the crucial computations they perform, and the features they represent, in the course of ICLL. Our analysis uses three complementary strategies:

- (a) **Attention visualization** to interpret the role of individual Transformer sub-components in solving REGBENCH. We find that Transformers develop “n-gram heads” that attend to the next token after contexts matching the current context window.
- (b) **Probing of hidden representations** to determine where (and how reliably) n-gram statistics are stored. We find that many sequence models learn to encode unigram counts, but Transformers more accurately encode higher-order n-gram statistics.
- (c) **Black-box input-output analysis** to evaluate behavioral similarity between Transformers and other learning algorithms known to be effective at ICLL. We find that smaller Transformers are well-approximated by 2-gram models, whereas larger transformers are closer to 3-gram models. We further find that n-gram models with learned smoothing (obtained by feeding n-gram statistics as input to an MLP-based neural predictor) also perform well at ICLL, and closely matches the behavior of large transformers.

While attention visualization, black-box analysis, and probing all have limitations as interpretability tools (Wen et al., 2023, Bolukbasi et al., 2021, Belinkov, 2022), the three methods provide convergent evidence that n-gram statistics play a key role in ICLL in transformers. Each of these findings is discussed in more detail below; in Section 6, we use them to motivate architectural changes that improve the behavior of transformers and other sequence models on both ICLL and natural language modeling tasks.

5.1 Transformers form in-context n-gram matching heads

Setup We visualize the attention weights of an (8-layer, 1-head) Transformer model on the test sequences from REGBENCH. In Figure 4, we plot attention weights between tokens in each layer using heatmaps for an example sequence in the early time steps ($i = 50 : 80$). Each row shows which tokens the label in that row attends to and the corresponding weights. We display the current DFA state next to each token label on the y and x axes.

Results The layer 2 and layer 3 attention heads each attend to the previous token. When composed, these heads enable each hidden representation (starting in layer 3) to incorporate information about the identities of the two tokens that precede it. The layer 5 head then appears to attend to tokens *following* 2-grams matching the most recent 2-gram in the input. In Figure 4, for example, the input ends in nh , and the layer 5 head attends to all tokens X in contexts nhX . More generally, on inputs of the form $ABC \cdots AB$, we observe that this head attends to tokens in the C position. Notably, these heads do not appear to selectively attend to tokens generated in the same DFA state, as might be expected in a model that is inferring the true data-generating process in context.

The pattern shown in Figure 4 is a higher-order analog of the “induction heads” previously described by Olsson et al. (2022). Versions of these heads identified in real models have been found to match a single context token; as described by Elhage et al. (2021), they require a circuit containing a single previous-token head (like our layer 2) followed by a context-matching head (like our layer 5). By composing multiple previous-token heads in series, models are able to match longer contexts.

5.2 Transformers represent in-context n-gram counts better than other models

The visualization above shows an attention pattern that is in principle compatible with computation of in-context n-gram statistics, but does not show that this is the quantity these heads in fact compute. In this section, we probe the hidden representations in this model (Shi et al., 2016) to determine whether the relevant quantities are encoded by models.

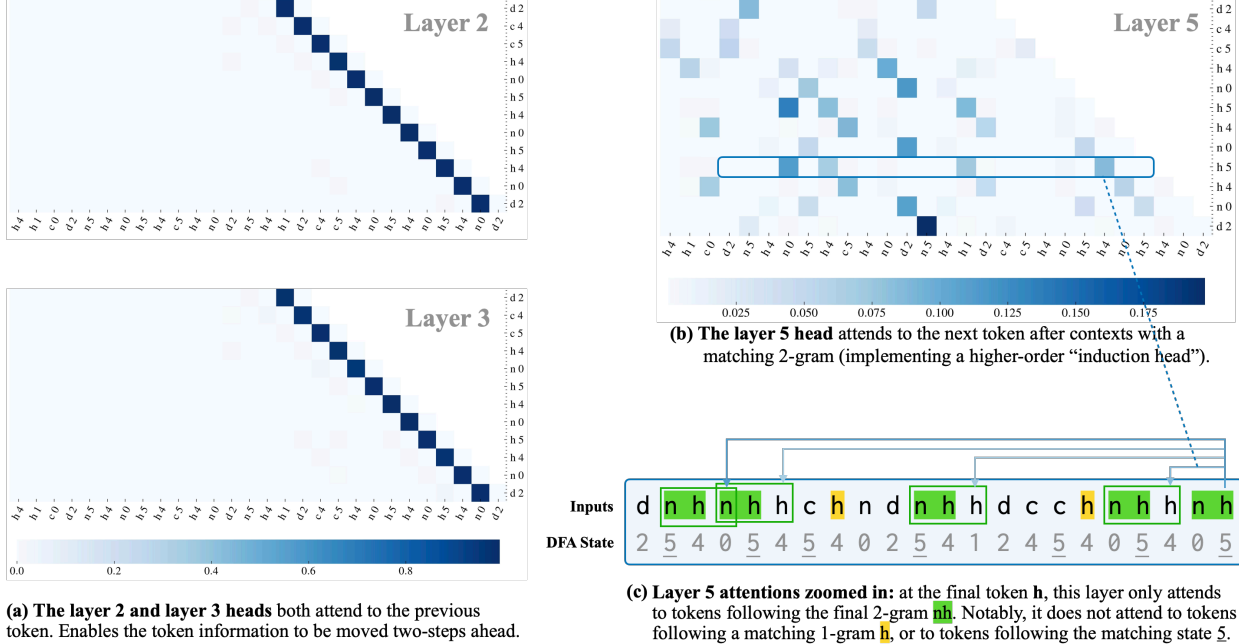


Figure 4: **N-gram heads in Transformers.** We plot the attention weights of an 8-layer, 1-head Transformer model trained on ICLL with $N = 2500$ training examples. Heads in early layers attend to previous tokens (a, b), while the attention head in layer 5 selectively attends to tokens based on 2-gram prefix match rather than the 1-gram match (the original induction head pattern) or the generator DFA’s current state.

Setup To train **n-gram probes**, we extract the intermediate layer outputs \mathbf{h} from the models as they process sequences from the training set. For varying values of n , we construct an MLP-based probe that takes as input a representation \mathbf{h}_i at time step i and a query token c . We train this probe to predict the (unnormalized) **count** of times c occurs following the same $n - 1$ tokens that appear at position i in the input. We then train similar probes to predict the (normalized) **frequency** $p(c | \mathbf{x}_{i-n+1}^i) = \frac{\text{count}(\mathbf{x}_{i-n+1}^i c)}{\text{count}(\mathbf{x}_{i-n+1}^i)}$ and the binary **existence** $\mathbf{1}[\text{count}(\mathbf{x}_{i-n+1}^i c) > 0]$.

We additionally probe models for whether they encode latent DFA states in their hidden representations. Because the labeling of states is arbitrary, we train these **state equivalence probes** to take two representations from different timesteps, and predict whether they were generated by the same underlying DFA state.

Implementation details and training hyperparameters for probes are described in more detail in Appendix E.

Metrics We evaluate count and frequency probes according to their relative error ($\frac{|\hat{y}-y|}{y}$; lower is better). We evaluate existence and state equivalence probes according to their binary classification accuracy (higher is better). We train separate probe models per layer, per model and per task. In Figure 5, we display the result for each task and model at the **best** layer.

Results The results in Figure 5 reveal clear patterns in the information recoverable from models’ hidden representations. All models encode normalized unigram frequencies with reasonably low error, though Transformers appear to do so slightly better. For larger context sizes (2-grams and 3-grams), probes on transformers substantially outperform probes trained on other models—generally the larger the Transformer the better the 3-gram performance. Interestingly, however, these results do not carry over to unnormalized counts, for which transformer encodings do not seem to be meaningfully different from other architectures.

In addition to counts, we can recover transformers an n-gram’s presence (Figure 5b) more accurately than other models, followed by RetNet and Mamba. More importantly, Transformers hidden states are not just better representative of n-gram features but we can also probe the equivalence of underlying automata states better compared to other model architectures (Figure 5c). We also provide additional results for the models trained with high resource settings in Figure 7, with similar findings. Supplementary results for models trained under high-resource conditions are presented in Figure 7.

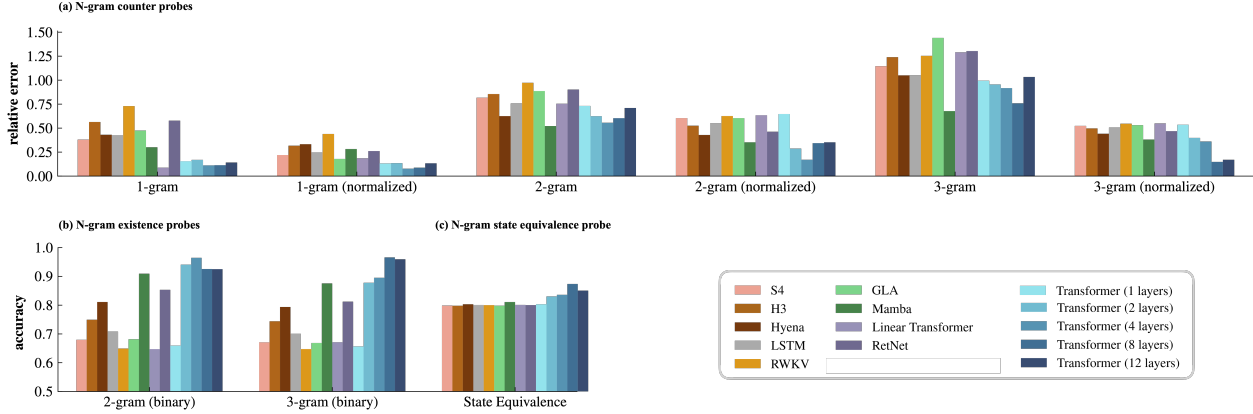


Figure 5: **Probing analysis of n-gram representations in neural sequence models** (trained with $N_{\text{train}} = 2500$ examples): (a) Probes are trained to predict the counts and frequencies of the most recent $(n-1)$ -gram + a next query character from the model’s hidden state at that time step. Results indicate that Transformer architectures more effectively encode frequencies of higher-order n-grams (bi-grams and tri-grams) compared to other models, with larger Transformer models exhibiting improved performance for higher n-grams. (b) Additional probes assess the ability to detect the presence of an n-gram, revealing that Transformers are superior in this task and in determining state equivalence (c).

5.3 Transformer predictions resemble n-gram models with learned reweighting

The previous two sections describe a flow of information through Transformer models consistent with the hypothesis that Transformer ICLL relies on computation of in-context n-gram statistics. However, it does not explain how models use this information to *predict* a distribution over next tokens. Here, we show that Transformer predictions are also well approximated by those of simpler models with access to the context *only* via n-gram statistics.

Setup The experiments in Section 4 compared the accuracy of transformer predictions to standard smoothed 2- and 3-gram models, as well as unsupervised DFA induction. There we observed that Transformers, trained on enough data, more accurately predicted the distribution over next tokens than n-gram language models. Here, we compare these different models’ predictions *to each other*, in addition to the ground-truth language. In doing so, we aim to reveal similarities in prediction strategies across predictors of very different classes.

In addition to the Transformers, other neural sequence models, and symbolic baselines, we introduce one new model for comparison: a **learned n-gram reweighting** model. Given an input sequence, we this model first computes a fixed feature representation of this input sequence by computing the empirical next-token distribution in contexts matching the last 1 and 2 tokens of the input, as well as the empirical unigram distribution. It then concatenates these distributions and passes them through an MLP with one hidden layer. This model is trained using the language modeling objective in Equation (1), on the same data as other models. We evaluate two variants of this model: one in which the input feature representation contains unnormalized counts of matching n-grams, and another in which the input contains normalized distributions. In automata-theoretic terms, this model may be viewed as a kind of counter automaton (Merrill, 2020).

These comparisons are shown in Figure 6.

Results Large Transformers with many layers tend to produce next-token distributions more similar to those of n-gram models than to the ground truth DFA or the Baum-Welch algorithm. Specifically, the average total variation distance (TVD) between the large Transformer’s predictions and the 3-gram model is 0.21, compared to 0.31 for the Baum-Welch learner (BW), and 0.36 for the next-token distribution in the ground truth language (GT). Moreover, the learned n-gram reweighting model (LNW_r) best approximates the distributions from the large Transformer, with a TVD of 0.16. This suggests the Transformer may implement an implicit smoothing mechanism similar to this learned approach. Interestingly (and in line with the findings in Section 5.1) the shallow 2-layer Transformer more closely matches predictions from the 2-gram baseline (TVD of 0.2) than the 3-gram baseline (TVD of 0.25).

In summary, our experiments show that Transformers compute next token distributions more similar to those of smoothed n-gram models than other neural sequence models.

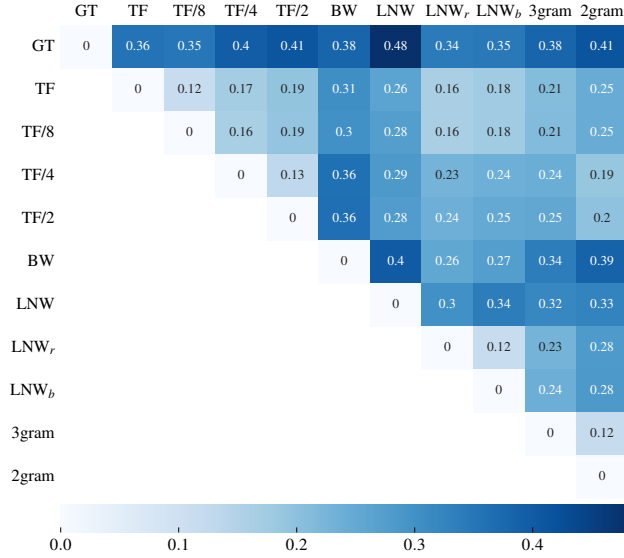


Figure 6: **Pairwise total variation distance (TVD) over first 100 characters:** We measure total variation distance between pairs of models (trained with $N = 2500$ examples) or algorithms across the first 100 tokens of the REGBENCH test set. We find that outputs of the 12-layer Transformer model (TF) are closest to the learned MLP reweighter model with normalized in-context n-gram distributions as input (LNW_r). The 3-gram model is the second best match. In the shallow 2-layer Transformer (TF/2) are closer to 2-gram than 3-gram predictions.

6 How Can Findings About ICLL Inform the Design of Neural Sequence Models?

The previous section suggests that at least part of Transformers’ success on ICLL tasks is their ability to efficiently compute in-context n-gram statistics. Can we use this information to improve other models, or to make Transformers more efficient?

The attention pattern associated with “n-gram heads” (illustrated in layer 5 of Figure 4) may be parameterized as follows:

$$A(n)_{ij} \propto \mathbf{1}[\underbrace{(\bigwedge_{k=1}^n x_{i-k} = x_{j-k-1})}_{\text{n-gram matching}} \wedge \underbrace{(i > j)}_{\text{causal mask}}], \quad (12)$$

where A_{ij} denotes the weight with which the i th token attends to the j th token.

Building on this observation, we propose to equip models with special **static n-gram attention heads** (which attend in a fixed fashion, but apply a learned transformation of the attended-to representation) as follows:

$$\text{NGH}^n(h^{(l-1)})_t = W_1 \mathbf{h}_t^{(l-1)} + W_2 A(n)_t^\top \mathbf{h}^{(l-1)}, \quad (13)$$

For a model with a hidden state of size d , such a head has $2d^2$ parameters, and only requires two matrix multiplications. To improve a model, we can simply insert it as a standalone new layer between the original layers of an existing model.^{5,6}

Unlike a standard self-attention layer, NGHⁿ does not have to store the prefix in memory during model inference. This property makes it compatible with recurrent models. In particular, in-context ngrams can be compressed via trie (e.g., as in Pauls and Klein (2011)) and queried efficiently in both time and space. Thus, for models with recurrent form (e.g., GLA/RetNet/Mamba), NGHⁿ does not introduce much overhead at recurrent inference time.

We evaluate the usefulness of n-gram heads for both ICLL and natural language modeling problems.

Setup: ICLL Our experiments take an existing architecture (for example RetNet), and insert a sequence of three NGH heads with increasing context size [NGH¹, NGH², NGH³] sequentially. We denote this whole bundle as the NGH_m^(1,2,3),

⁵Concurrent work by Arora et al. (2023) also inserts sparse attention layers into non-transformer models from the perspective of efficiency. Their implementation is equivalent to our NGH¹, but with learned attention weights; our implementation attends uniformly to all matching contexts.

⁶For Transformer models, we may add these as additional heads in a multi-head attention mechanism.

(a) **n-gram layers bring other models to the Transformer level on ICLL:** We train RetNet and GLA models with n-gram heads on ICLL with $N = 2500$ training examples. In TVD metric, adding n-gram layers, brings model performance to the Transformer level trained on the same data without n-gram heads.. In accuracy, hybrid models can outperform Transformer models in the accuracy metric.

Model	TVD (\downarrow)	Accuracy (\uparrow)
RetNet (Sun et al., 2023)	0.392	0.800
\perp $\text{NGH}_1^{(1)}$	0.310	0.814
\perp $\text{NGH}_1^{(1,2)}$	0.229	0.925
\perp $\text{NGH}_1^{(1,2,3)}$	0.217	0.94
GLA (Yang et al., 2023)	0.624	0.526
\perp $\text{NGH}_1^{(1)}$	0.302	0.819
\perp $\text{NGH}_1^{(1,2)}$	0.211	0.929
\perp $\text{NGH}_1^{(1,2,3)}$	0.207	0.946
Transformer (Vaswani et al., 2017)	0.203	0.926

(b) **n-gram layers improves language models:** We train equal sized (340M parameters) language models with and without n-gram heads on 7B tokens from the SlimPajama dataset (Soboleva et al., 2023). Adding n-gram layers improves each models performance regardless of the model by reducing test set perplexities up to 1.14 point.

Model	Perplexity (\downarrow)
RetNet (Sun et al., 2023)	16.55
\perp $\text{NGH}_1^{(1,2,3)} + \text{NGH}_{23}^{(1,2,3)}$	15.86 (+4.2%)
GLA (Yang et al., 2023)	15.65
\perp $\text{NGH}_1^{(1,1,1)} + \text{NGH}_{23}^{(1,1,1)}$	15.54 (+0.7%)
\perp $\text{NGH}_1^{(1,2,3)} + \text{NGH}_{23}^{(1,2,3)}$	15.24 (+2.6%)
Transformer (Llama) (Touvron et al., 2023)	16.96
\perp $\text{NGH}_1^{(1,2,3)} + \text{NGH}_{23}^{(1,2,3)}$	15.82 (+6.7%)

Table 1: Hybrid model experiments on ICLL and language modeling.

where m specifies the original layer after which the NGH heads are added, and the whole architecture as RetNet + $\text{NGH}_m^{(1,2,3)}$.

Results: ICLL We experiment by inserting n-gram layers to the base RetNet and GLA models. In Table 1(a), the addition of the original induction heads ($\text{NGH}^{(1)}$) improves GLA more than 50% in TVD, and improves RetNet slightly. After adding the second order induction heads ($\text{NGH}^{(1,2)}$), both RetNet and GLA match Transformer performance. Adding third order induction heads improves the performance even further, enabling the models to outperform the Transformer in the accuracy metric.

Setup: Language Modeling We next explore whether improvements in ICLL transfer over to language modeling on real data.

In these language modeling experiments, we additionally add MLP network after the sequence of NGH layers such that $\text{NGH}_m^{(1,2,3)}$ plus MLP makes $12d^2$ parameters, matching the number of parameters in ordinary base model layers. For each base model, we experiment with inserting two n-gram head sequences: one replacing the second layer ($\text{NGH}_1^{(1,2,3)}$), and one replacing the second-to-last layer ($\text{NGH}_{23}^{(1,2,3)}$).

Results: Language Modeling In Table 1(b), we show that n-gram heads consistently improve language models. Indeed, the best improvement comes from the Transformer model itself, with a 6.7% decrease in the perplexity. We also evaluate whether higher-order n-gram heads are really necessary, by evaluating GLA with only 1-gram layers; using all n-grams decreases perplexity 4 times more than using just 1-gram layers (5th row).

The consistent improvements in our setting indicate that n-gram head is one of the mechanisms current sequence models not good at learning from language modeling data itself particularly at 340M parameter scale. Recent work (Arora et al., 2023) has shown 1-gram versions of these layers being helpful in synthetic datasets: we show that higher order ($n > 1$) n-gram heads extends these improvements to real language modeling in a diverse set of neural sequence models, including Transformers itself.

7 Conclusion

In this work, we have proposed a new family of model problems we call in-context language learning (ICLL) that captures important challenges for in-context learning with large language models in real-world settings. Through analysis of model performance on this task, we have identified key differences among classes of neural sequence models, with Transformers emerging as particularly adept at in-context learning. Further investigation has revealed that Transformers succeed by implementing in-context n-gram heads (higher-order induction heads). Inspired by these findings, we demonstrated that inserting simple induction heads for n-gram modeling into neural architectures

significantly improves their ICLL performance as well as their language modeling abilities in natural data. In a broader scope, this paper provides evidence supporting the hypothesis that real language models can in-context learn using known learning algorithms.

Acknowledgements

We thank William Merrill for valuable feedback on an early draft of this paper. Ekin Akyürek and Jacob Andreas are supported by Intel and the National Science Foundation under the PPOSS program (CCF-2217064) as well as the OpenPhilanthropy Foundation. Yoon Kim and Bailin Wang were supported by MIT-IBM Watson AI.

References

- Ekin Akyürek, Dale Schuurmans, Jacob Andreas, Tengyu Ma, and Denny Zhou. What learning algorithm is in-context learning? investigations with linear models. *ArXiv preprint*, abs/2211.15661, 2022. URL <https://arxiv.org/abs/2211.15661>.
- Simran Arora, Sabri Eyuboglu, Aman Timalsina, Isys Johnson, Michael Poli, James Zou, Atri Rudra, and Christopher Ré. Zoology: Measuring and improving recall in efficient language models. *ArXiv preprint*, abs/2312.04927, 2023. URL <https://arxiv.org/abs/2312.04927>.
- Yonatan Belinkov. Probing classifiers: Promises, shortcomings, and advances. *Computational Linguistics*, 48(1): 207–219, 2022. doi:10.1162/coli_a_00422. URL <https://aclanthology.org/2022.cl-1.7>.
- Satwik Bhattamishra, Kabir Ahuja, and Navin Goyal. On the Ability and Limitations of Transformers to Recognize Formal Languages. In *Proceedings of the 2020 Conference on Empirical Methods in Natural Language Processing (EMNLP)*, pages 7096–7116, Online, 2020. Association for Computational Linguistics. doi:10.18653/v1/2020.emnlp-main.576. URL <https://aclanthology.org/2020.emnlp-main.576>.
- Satwik Bhattamishra, Arkil Patel, Phil Blunsom, and Varun Kanade. Understanding in-context learning in transformers and llms by learning to learn discrete functions. *ArXiv preprint*, abs/2310.03016, 2023. URL <https://arxiv.org/abs/2310.03016>.
- Tolga Bolukbasi, Adam Pearce, Ann Yuan, Andy Coenen, Emily Reif, Fernanda Viégas, and Martin Wattenberg. An interpretability illusion for bert. *ArXiv preprint*, abs/2104.07143, 2021. URL <https://arxiv.org/abs/2104.07143>.
- Stephanie Chan, Adam Santoro, Andrew Lampinen, Jane Wang, Aaditya Singh, Pierre Richemond, James McClelland, and Felix Hill. Data distributional properties drive emergent in-context learning in transformers. *Advances in Neural Information Processing Systems*, 35:18878–18891, 2022.
- Stanley F. Chen and Joshua Goodman. An empirical study of smoothing techniques for language modeling. In *34th Annual Meeting of the Association for Computational Linguistics*, pages 310–318, Santa Cruz, California, USA, 1996. Association for Computational Linguistics. doi:10.3115/981863.981904. URL <https://aclanthology.org/P96-1041>.
- Damai Dai, Yutao Sun, Li Dong, Yaru Hao, Shuming Ma, Zhifang Sui, and Furu Wei. Why can gpt learn in-context? language models secretly perform gradient descent as meta-optimizers. In *Findings of the Association for Computational Linguistics: ACL 2023*, pages 4005–4019, 2023.
- Tri Dao, Daniel Y Fu, Khaled K Saab, Armin W Thomas, Atri Rudra, and Christopher Ré. Hungry hungry hippos: Towards language modeling with state space models. *ArXiv preprint*, abs/2212.14052, 2022. URL <https://arxiv.org/abs/2212.14052>.
- Arthur P Dempster, Nan M Laird, and Donald B Rubin. Maximum likelihood from incomplete data via the em algorithm. *Journal of the royal statistical society: series B (methodological)*, 39(1):1–22, 1977.
- Andrew Drozdov, Nathanael Schärli, Ekin Akyürek, Nathan Scales, Xinying Song, Xinyun Chen, Olivier Bousquet, and Denny Zhou. Compositional semantic parsing with large language models. *ArXiv preprint*, abs/2209.15003, 2022. URL <https://arxiv.org/abs/2209.15003>.
- P. Dupont, F. Denis, and Y. Esposito. Links between probabilistic automata and hidden markov models: probability distributions, learning models and induction algorithms. *Pattern Recognition*, 38(9):1349–1371, 2005. ISSN 0031-3203. doi:<https://doi.org/10.1016/j.patcog.2004.03.020>. URL <https://www.sciencedirect.com/science/article/pii/S0031320305000233>. Grammatical Inference.

- Nelson Elhage, Neel Nanda, Catherine Olsson, Tom Henighan, Nicholas Joseph, Ben Mann, Amanda Askell, Yuntao Bai, Anna Chen, Tom Conerly, et al. A mathematical framework for transformer circuits. *Transformer Circuits Thread*, 1, 2021.
- Jeffrey L Elman. Finding structure in time. *Cognitive science*, 14(2):179–211, 1990.
- Matthew Finlayson, Kyle Richardson, Ashish Sabharwal, and Peter Clark. What makes instruction learning hard? an investigation and a new challenge in a synthetic environment. *arXiv preprint arXiv:2204.09148*, 2022.
- Shivam Garg, Dimitris Tsipras, Percy S Liang, and Gregory Valiant. What can transformers learn in-context? a case study of simple function classes. *Advances in Neural Information Processing Systems*, 35:30583–30598, 2022.
- Felix A Gers and E Schmidhuber. Lstm recurrent networks learn simple context-free and context-sensitive languages. *IEEE transactions on neural networks*, 12(6):1333–1340, 2001.
- E Mark Gold. Language identification in the limit. *Information and control*, 10(5):447–474, 1967.
- Albert Gu and Tri Dao. Mamba: Linear-time sequence modeling with selective state spaces. *ArXiv preprint, abs/2312.00752*, 2023. URL <https://arxiv.org/abs/2312.00752>.
- Albert Gu, Karan Goel, Ankit Gupta, and Christopher Ré. On the parameterization and initialization of diagonal state space models. *Advances in Neural Information Processing Systems*, 35:35971–35983, 2022a.
- Albert Gu, Karan Goel, and Christopher Ré. Efficiently modeling long sequences with structured state spaces. In *The Tenth International Conference on Learning Representations, ICLR 2022, Virtual Event, April 25-29, 2022*. OpenReview.net, 2022b. URL <https://openreview.net/forum?id=uYLFoz1v1AC>.
- Michael Hahn and Navin Goyal. A theory of emergent in-context learning as implicit structure induction. *ArXiv preprint, abs/2303.07971*, 2023. URL <https://arxiv.org/abs/2303.07971>.
- John Hewitt, Michael Hahn, Surya Ganguli, Percy Liang, and Christopher D. Manning. RNNs can generate bounded hierarchical languages with optimal memory. In *Proceedings of the 2020 Conference on Empirical Methods in Natural Language Processing (EMNLP)*, pages 1978–2010, Online, 2020. Association for Computational Linguistics. doi:10.18653/v1/2020.emnlp-main.156. URL <https://aclanthology.org/2020.emnlp-main.156>.
- Sepp Hochreiter and Jürgen Schmidhuber. Long short-term memory. *Neural computation*, 9(8):1735–1780, 1997.
- John Hopcroft. An $n \log n$ algorithm for minimizing states in a finite automaton. In *Theory of machines and computations*, pages 189–196. Elsevier, 1971.
- Weizhe Hua, Zihang Dai, Hanxiao Liu, and Quoc V. Le. Transformer quality in linear time. In Kamalika Chaudhuri, Stefanie Jegelka, Le Song, Csaba Szepesvári, Gang Niu, and Sivan Sabato, editors, *International Conference on Machine Learning, ICML 2022, 17-23 July 2022, Baltimore, Maryland, USA*, volume 162 of *Proceedings of Machine Learning Research*, pages 9099–9117. PMLR, 2022. URL <https://proceedings.mlr.press/v162/hua22a.html>.
- Angelos Katharopoulos, Apoorv Vyas, Nikolaos Pappas, and François Fleuret. Transformers are rnns: Fast autoregressive transformers with linear attention. In *Proceedings of the 37th International Conference on Machine Learning, ICML 2020, 13-18 July 2020, Virtual Event*, volume 119 of *Proceedings of Machine Learning Research*, pages 5156–5165. PMLR, 2020. URL <http://proceedings.mlr.press/v119/katharopoulos20a.html>.
- Harsh Mehta, Ankit Gupta, Ashok Cutkosky, and Behnam Neyshabur. Long range language modeling via gated state spaces. *arXiv preprint arXiv:2206.13947*, 2022.
- William Merrill. Sequential neural networks as automata. In *Proceedings of the Workshop on Deep Learning and Formal Languages: Building Bridges*, pages 1–13, Florence, 2019. Association for Computational Linguistics. doi:10.18653/v1/W19-3901. URL <https://aclanthology.org/W19-3901>.
- William Merrill. On the linguistic capacity of real-time counter automata. *arXiv preprint arXiv:2004.06866*, 2020.
- William Merrill and Ashish Sabharwal. The parallelism tradeoff: Limitations of log-precision transformers. *Transactions of the Association for Computational Linguistics*, 11:531–545, 2023.
- Sewon Min, Xinxu Lyu, Ari Holtzman, Mikel Artetxe, Mike Lewis, Hannaneh Hajishirzi, and Luke Zettlemoyer. Rethinking the role of demonstrations: What makes in-context learning work? *ArXiv preprint, abs/2202.12837*, 2022. URL <https://arxiv.org/abs/2202.12837>.
- Catherine Olsson, Nelson Elhage, Neel Nanda, Nicholas Joseph, Nova DasSarma, Tom Henighan, Ben Mann, Amanda Askell, Yuntao Bai, Anna Chen, et al. In-context learning and induction heads. *ArXiv preprint, abs/2209.11895*, 2022. URL <https://arxiv.org/abs/2209.11895>.
- Adam Pauls and Dan Klein. Faster and smaller n-gram language models. In *Proceedings of the 49th annual meeting of the Association for Computational Linguistics: Human Language Technologies*, pages 258–267, 2011.

- Bo Peng, Eric Alcaide, Quentin Anthony, Alon Albalak, Samuel Arcadinho, Huanqi Cao, Xin Cheng, Michael Chung, Matteo Grella, Kranthi Kiran GV, et al. Rvk: Reinventing rns for the transformer era. *ArXiv preprint*, abs/2305.13048, 2023. URL <https://arxiv.org/abs/2305.13048>.
- Michael Poli, Stefano Massaroli, Eric Nguyen, Daniel Y Fu, Tri Dao, Stephen Baccus, Yoshua Bengio, Stefano Ermon, and Christopher Ré. Hyena hierarchy: Towards larger convolutional language models. *ArXiv preprint*, abs/2302.10866, 2023. URL <https://arxiv.org/abs/2302.10866>.
- Zhen Qin, Xiaodong Han, Weixuan Sun, Dongxu Li, Lingpeng Kong, Nick Barnes, and Yiran Zhong. The devil in linear transformer. *ArXiv preprint*, abs/2210.10340, 2022. URL <https://arxiv.org/abs/2210.10340>.
- Lawrence R Rabiner. A tutorial on hidden markov models and selected applications in speech recognition. *Proceedings of the IEEE*, 77(2):257–286, 1989.
- Xing Shi, Inkit Padhi, and Kevin Knight. Does string-based neural MT learn source syntax? In *Proceedings of the 2016 Conference on Empirical Methods in Natural Language Processing*, pages 1526–1534, Austin, Texas, 2016. Association for Computational Linguistics. doi:10.18653/v1/D16-1159. URL <https://aclanthology.org/D16-1159>.
- Richard Shin and Benjamin Van Durme. Few-shot semantic parsing with language models trained on code. In *Proceedings of the 2022 Conference of the North American Chapter of the Association for Computational Linguistics: Human Language Technologies*, pages 5417–5425, Seattle, United States, 2022. Association for Computational Linguistics. doi:10.18653/v1/2022.naacl-main.396. URL <https://aclanthology.org/2022.naacl-main.396>.
- Daria Soboleva, Faisal Al-Khateeb, Robert Myers, Jacob R Steeves, Joel Hestness, and Nolan Dey. SlimPajama: A 627B token cleaned and deduplicated version of RedPajama. <https://www.cerebras.net/blog/slimpajama-a-627b-token-cleaned-and-deduplicated-version-of-redpajama>, 2023. URL <https://huggingface.co/datasets/cerebras/SlimPajama-627B>.
- Jianlin Su, Murtadha Ahmed, Yu Lu, Shengfeng Pan, Wen Bo, and Yunfeng Liu. Roformer: Enhanced transformer with rotary position embedding. *Neurocomputing*, 568:127063, 2024.
- Yutao Sun, Li Dong, Shaohan Huang, Shuming Ma, Yuqing Xia, Jilong Xue, Jianyong Wang, and Furu Wei. Retentive network: A successor to transformer for large language models. *ArXiv preprint*, abs/2307.08621, 2023. URL <https://arxiv.org/abs/2307.08621>.
- Mirac Suzgun, Sebastian Gehrmann, Yonatan Belinkov, and Stuart M Shieber. Memory-augmented recurrent neural networks can learn generalized dyck languages. *ArXiv preprint*, abs/1911.03329, 2019. URL <https://arxiv.org/abs/1911.03329>.
- Hugo Touvron, Thibaut Lavril, Gautier Izacard, Xavier Martinet, Marie-Anne Lachaux, Timothée Lacroix, Baptiste Rozière, Naman Goyal, Eric Hambro, Faisal Azhar, et al. Llama: Open and efficient foundation language models. *ArXiv preprint*, abs/2302.13971, 2023. URL <https://arxiv.org/abs/2302.13971>.
- Ashish Vaswani, Noam Shazeer, Niki Parmar, Jakob Uszkoreit, Llion Jones, Aidan N. Gomez, Lukasz Kaiser, and Illia Polosukhin. Attention is all you need. In Isabelle Guyon, Ulrike von Luxburg, Samy Bengio, Hanna M. Wallach, Rob Fergus, S. V. N. Vishwanathan, and Roman Garnett, editors, *Advances in Neural Information Processing Systems 30: Annual Conference on Neural Information Processing Systems 2017, December 4-9, 2017, Long Beach, CA, USA*, pages 5998–6008, 2017. URL <https://proceedings.neurips.cc/paper/2017/hash/3f5ee243547dee91fbd053c1c4a845aa-Abstract.html>.
- Johannes von Oswald, Eyvind Niklasson, Ettore Randazzo, João Sacramento, Alexander Mordvintsev, Andrey Zhmoginov, and Max Vladymyrov. Transformers learn in-context by gradient descent. In *International Conference on Machine Learning*, pages 35151–35174. PMLR, 2023a.
- Johannes von Oswald, Eyvind Niklasson, Maximilian Schlegel, Seijin Kobayashi, Nicolas Zucchet, Nino Scherrer, Nolan Miller, Mark Sandler, Max Vladymyrov, Razvan Pascanu, et al. Uncovering mesa-optimization algorithms in transformers. *ArXiv preprint*, abs/2309.05858, 2023b. URL <https://arxiv.org/abs/2309.05858>.
- Jerry Wei, Jason Wei, Yi Tay, Dustin Tran, Albert Webson, Yifeng Lu, Xinyun Chen, Hanxiao Liu, Da Huang, Denny Zhou, et al. Larger language models do in-context learning differently. *ArXiv preprint*, abs/2303.03846, 2023. URL <https://arxiv.org/abs/2303.03846>.
- Kaiyue Wen, Yuchen Li, Bingbin Liu, and Andrej Risteski. Transformers are uninterpretable with myopic methods: a case study with bounded dyck grammars. *ArXiv preprint*, abs/2312.01429, 2023. URL <https://arxiv.org/abs/2312.01429>.
- Sang Michael Xie, Aditi Raghunathan, Percy Liang, and Tengyu Ma. An explanation of in-context learning as implicit bayesian inference. In *The Tenth International Conference on Learning Representations, ICLR 2022, Virtual Event, April 25-29, 2022*. OpenReview.net, 2022. URL <https://openreview.net/forum?id=RdJVFCHJUMI>.

Songlin Yang, Bailin Wang, Yikang Shen, Rameswar Panda, and Yoon Kim. Gated linear attention transformers with hardware-efficient training. *ArXiv preprint*, abs/2312.06635, 2023. URL <https://arxiv.org/abs/2312.06635>.

Shuangfei Zhai, Walter Talbott, Nitish Srivastava, Chen Huang, Hanlin Goh, Ruixiang Zhang, and Josh Susskind. An attention free transformer. *ArXiv preprint*, abs/2105.14103, 2021. URL <https://arxiv.org/abs/2105.14103>.

A Model Architectures

We experiment with a set of neural autoregressive sequence models that model the generative process of a sequence via $\prod_{i=1}^T p_m(\mathbf{x}_{i+1} | \mathbf{x}_{1:i})$. We characterize each model with three common consecutive modules: (i) an **embedding layer** that maps input tokens to vectors, (ii) a stack of **backbone layers**, (iii) and an **output projection** layer that maps the final outputs from the backbone to the distribution over the token space.

$$p_m(\mathbf{x}_{i+1} | \mathbf{x}_{1:i}) = \text{softmax}(m_{\text{output}} \circ m_{\text{backbone}} \circ m_{\text{embed}}(\mathbf{x}_{1:i})) \quad (14)$$

Collectively, the three modules form a mapping from one-hot vectors to pre-softmax logits, i.e., $\{0, 1\}^{T \times |V|} \rightarrow \mathbb{R}^{T \times |V|}$ where T denotes the sequence length, $|V|$ denotes the vocabulary size.

Embedding Layer (m_{embed}) The embedding layer is a single projection matrix which converts one-hot input vectors to dense vectors:

$$m_{\text{embed}}(\mathbf{x}) = \mathbf{W}_e \mathbf{x}. \quad (15)$$

In almost all models, the positional information need not be incorporated in the embedding layer. It is either explicitly added as the rotary positional embeddings (Rope, Su et al. (2024)) in the attention layer, or implicitly handled in the recurrence/convolution form of models. The only exception is the original Transformer with multi-head attention, where positional information is added as learnt positional embeddings:

$$m_{\text{embed}}(\mathbf{x})_i = \mathbf{W}_e \mathbf{x}_i + \mathbf{W}_p \mathbf{i}, \quad (16)$$

where \mathbf{i} is one-hot representation of the time-step t . We use the original Transformer in our synthetic experiments, and use the improved Transformer with Rope in our language modelling experiments on real data.

Backbone Layers ($m_{\text{backbone}}^{(l)}$) Each backbone layer updates the previous layer’s hidden outputs ($\mathbf{h}^{(l-1)}$) in two sequential steps. First, a **token mixer** that models the token-level interactions. Effectively, it can be any *causal* network mapping hidden states of previous tokens to a new hidden state for the current token:

$$\mathbf{a}^{(l)} = m_{\text{mixer}}^{(l)}(\mathbf{h}^{(l-1)}), \quad (17)$$

where $m_{\text{mixer}}^{(l)}(\mathbf{h}^{(l-1)})_i = m_{\text{mixer}}^{(l)}(\mathbf{h}_{1:i}^{(l-1)})_t$. Then, a **feed-forward** network, $m_{\text{FF}}^{(l)}$, applied to the final outputs of the layer with a residual connection:

$$m_{\text{backbone}}^{(l)}(\mathbf{h}^{(l-1)}) = m_{\text{FF}}^{(l)}(\mathbf{a}^{(l)}) + \mathbf{a}^{(l)}. \quad (18)$$

or alternatively in a gated-linear unit (GAU, Hua et al. (2022)) structure:

$$m_{\text{backbone}}^{(l)}(\mathbf{h}^{(l-1)}) = m_{\text{GAU}}^{(l)}(\mathbf{h}^{(l-1)}, \mathbf{a}^{(l)}) + \mathbf{a}^{(l)}. \quad (19)$$

where $m_{\text{GAU}}(\mathbf{x}, \mathbf{y}) = \mathbf{W}_3(\mathbf{W}_1 \mathbf{x}) \odot (\mathbf{W}_2 \mathbf{y})$, and \odot denotes element-wise product.⁷ In contrast to the token mixer, the feed-forward network is applied individually for each token, i.e., there is no token-wise interactions.

Output Projection (m_{output}) The projection layer consists of a single fully-connected projection that converts the outputs of the backbone $\mathbf{h}^{(L)}$ to the output space:

$$m_{\text{output}}(\mathbf{h}^{(L)}) = \mathbf{W}_o \mathbf{h}^{(L)} \quad (20)$$

In the following sections, we review the model architectures studied in this work - they share the common skeleton presented above, and mainly differ in the design of the token-mixing module m_{mixer} .⁸ We intend to present a unified view of all models by using shared notations and equivalent forms (when possible).

We will denote input/output of a token mixer as $\mathbf{x} \in \mathbb{R}^{L \times d}$ and $\mathbf{y} \in \mathbb{R}^{L \times d}$, respectively. When possible, we will present all the possible forms (i.e., attention-style form, recurrent form and convolutional form) of a model. Generally, attention-style/convolutional forms are useful for developing training schema, whereas recurrent forms are crucial for model’s inference schema.

⁷Among all the models presented, only Mamba employs the GAU architecture.

⁸For brevity, we omit the normalization layers which are applied before each token mixer and feed-forward layer.

A.1 Transformers with Self Attention (Vaswani et al., 2017)

Standard self-attention performs token mixing in the following way:

$$\mathbf{q}_i, \mathbf{k}_j = \mathbf{W}_q \mathbf{x}_i, \mathbf{W}_k \mathbf{x}_j \in \mathbb{R}^{d_k} \quad (21)$$

$$\mathbf{A}_{ij} \propto \exp(\langle \mathbf{q}_i, \mathbf{k}_j \rangle) \in (0, 1) \quad \text{softmax attention} \quad (22)$$

$$\mathbf{v}_j = \mathbf{W}_v \mathbf{x}_j \in \mathbb{R}^{d_v} \quad (23)$$

$$\mathbf{z}_i = \sum_{j=1}^i \mathbf{A}_{ij} \mathbf{v}_j \in \mathbb{R}^{d_v} \quad (24)$$

$$\mathbf{y}_i = \mathbf{W}_o \mathbf{z}_i \in \mathbb{R}^d \quad (25)$$

where d_k, d_v denote the dimension for query/key and value vectors, respectively. The attention scores are computed based on the pairwise dot-product between the query vector of the current token and key vectors from the context. In the multi-head attention, attention output \mathbf{z}_i is independently computed in each head; all outputs are concatenated as the final attention output, which will then be fed into the output projection \mathbf{W}_o .

A.2 Transformers with Linear Attention (Katharopoulos et al., 2020)

The linear attention (Katharopoulos et al., 2020) simplifies the standard attention by replacing $\exp(\langle \mathbf{q}_i, \mathbf{k}_j \rangle)$ with a kernel map $k(\mathbf{q}_i, \mathbf{k}_j)$ with an associative feature map (i.e., $k(\mathbf{q}_i, \mathbf{k}_j) = \phi(\mathbf{q}_i)\phi(\mathbf{k}_j)$). In this work, we consider a simple feature map of identity function (i.e., $\phi(\mathbf{q}_i) = \mathbf{q}_i$), which yields surprisingly good performance for language model on real data in recent works (Qin et al., 2022, Yang et al., 2023). With this feature map, the token mixing process is very similar to standard attention, except that attention scores are not normalized.

$$\mathbf{q}_i, \mathbf{k}_j = \mathbf{W}_q \mathbf{x}_i, \mathbf{W}_k \mathbf{x}_j \in \mathbb{R}^{d_k} \quad (26)$$

$$\mathbf{A}_{ij} = \langle \mathbf{q}_i, \mathbf{k}_j \rangle \quad \text{linear attention} \quad (27)$$

$$\mathbf{v}_j = \mathbf{W}_v \mathbf{x}_j \in \mathbb{R}^{d_v} \quad (28)$$

$$\mathbf{z}_i = \sum_{j=1}^i \mathbf{A}_{ij} \mathbf{v}_j \in \mathbb{R}^{d_v} \quad (29)$$

$$\mathbf{y}_i = \mathbf{W}_o \mathbf{z}_i \in \mathbb{R}^d \quad (30)$$

The linear attention has an equivalent recurrent form as follows.

$$\mathbf{q}_i, \mathbf{k}_j = \mathbf{W}_q \mathbf{x}_i, \mathbf{W}_k \mathbf{x}_j \in \mathbb{R}^{d_k} \quad (31)$$

$$\mathbf{S}_i = \mathbf{S}_{i-1} + \mathbf{k}_i^T \mathbf{v}_i \in \mathbb{R}^{d_k \times d_v} \quad (32)$$

$$\mathbf{z}_i = \mathbf{q}_i^T \mathbf{S}_i \in \mathbb{R}^{d_v} \quad (33)$$

(rest is the same as the attention form)

where \mathbf{S} is the 2-D hidden states of the linear recurrence.

A.3 RetNet (Sun et al., 2023, Qin et al., 2022)

Based on linear attention, RetNet⁹ further incorporates rotary positional embeddings (Su et al., 2024) and a fixed decay rate λ . The resulting token mixer, namely *retention*, has the following form.

$$\mathbf{q}_i, \mathbf{k}_j = \mathbf{W}_q \mathbf{x}_i, \mathbf{W}_k \mathbf{x}_j \in \mathbb{R}^{d_k} \quad (34)$$

$$\tilde{\mathbf{q}}_i, \tilde{\mathbf{k}}_j = \text{RoPE}(\mathbf{q}_{1:i}), \text{RoPE}(\mathbf{k}_{1:j}) \in \mathbb{R}^{d_k} \quad (35)$$

$$\mathbf{A}_{ij} = \lambda^{i-j} \langle \tilde{\mathbf{q}}_i, \tilde{\mathbf{k}}_j \rangle \quad (36)$$

$$\mathbf{v}_j = \mathbf{W}_v \mathbf{x}_j \in \mathbb{R}^{d_v} \quad (37)$$

$$\mathbf{z}_i = \text{retention}(\mathbf{x}_{1:i}) = \sum_{j=1}^i \mathbf{A}_{ij} \mathbf{v}_j \in \mathbb{R}^{d_v} \quad (38)$$

$$\mathbf{r}_i = \mathbf{W}_r \mathbf{x}_i \in \mathbb{R}^{d_v} \quad (39)$$

$$\mathbf{y}_i = \mathbf{W}_o (\text{swish}(\mathbf{r}_i) \odot \mathbf{z}_i) \in \mathbb{R}^d \quad (40)$$

While the addition of rotary positional embedding to query/key vectors is straightforward in this attention-style form, the additional decay term λ is easier to understand in this equivalent recurrent form. The linear attention has an equivalent recurrent form as follows.

$$\mathbf{q}_i, \mathbf{k}_j = \mathbf{W}_q \mathbf{x}_i, \mathbf{W}_k \mathbf{x}_j \in \mathbb{R}^{d_k} \quad (41)$$

$$\tilde{\mathbf{q}}_i, \tilde{\mathbf{k}}_j = \text{RoPE}(\mathbf{q}_{1:i}), \text{RoPE}(\mathbf{k}_{1:j}) \in \mathbb{R}^{d_k} \quad (42)$$

$$\mathbf{S}_i = \lambda \mathbf{S}_{i-1} + \tilde{\mathbf{k}}_i^\top \mathbf{v}_i \in \mathbb{R}^{d_k \times d_v} \quad (43)$$

$$\mathbf{z}_i = \tilde{\mathbf{q}}_i^\top \mathbf{S}_i \in \mathbb{R}^{d_v} \quad (44)$$

(rest is the same as the attention form)

A.4 LSTM (Hochreiter and Schmidhuber, 1997)

All the recurrences we presented are linear in that there are no non-linear dependencies between adjacent hidden states, e.g., $\partial \mathbf{S}_i / \partial \mathbf{S}_{i-1}$ is not a function of \mathbf{S}_{i-1} . For completeness of recurrences, we also consider LSTM (Hochreiter and Schmidhuber, 1997), which is widely used in the pre-Transformer era. LSTM uses the following non-linear recurrence,

$$\mathbf{f}_i = \sigma(\mathbf{W}_f \mathbf{x}_i + \mathbf{U}_f \mathbf{h}_{i-1}) \in \mathbb{R}^d \quad (45)$$

$$\mathbf{i}_i = \sigma(\mathbf{W}_i \mathbf{x}_i + \mathbf{U}_i \mathbf{h}_{i-1}) \in \mathbb{R}^d \quad (46)$$

$$\mathbf{o}_i = \sigma(\mathbf{W}_o \mathbf{x}_i + \mathbf{U}_o \mathbf{h}_{i-1}) \in \mathbb{R}^d \quad (47)$$

$$\tilde{\mathbf{c}}_i = \tanh(\mathbf{W}_c \mathbf{x}_i + \mathbf{U}_c \mathbf{h}_{i-1}) \in \mathbb{R}^d \quad (48)$$

$$\mathbf{c}_i = \mathbf{f}_i \odot \mathbf{c}_{i-1} + \mathbf{i}_i \odot \tilde{\mathbf{c}}_i \in \mathbb{R}^d \quad (49)$$

$$\mathbf{y}_i = \mathbf{o}_i \odot \tanh(\mathbf{c}_i) \in \mathbb{R}^d \quad (50)$$

where $\mathbf{f}, \mathbf{i}, \mathbf{o}$ denotes forget, input and output gate, respectively. To strictly follow the architecture of traditional multi-layer LSTM, we do not use the feed-forward in-between LSTM layers, i.e., the input of layer l is directly the output from layer $l-1$.

A.5 GLA (Yang et al., 2023)

Compared with RetNet, GLA incorporated more fine-grained data-dependent gating. Instead of using the rotary positional embedding, the fine-grained gates can implicitly capture positional information. For the ease of understanding, we first show the recurrent form of GLA, and then its attention-style form.

⁹TransNormer proposed in Qin et al. (2022) has almost the same architecture as RetNet.

For each token, GLA additionally relies on two data dependent decay vectors $\alpha_i \in \mathbb{R}^{d_k}$ and $\beta_i \in \mathbb{R}^{d_v}$. The outer-product of them (i.e., $\alpha_i^\top \beta_i$) decides how much information to preserve from previous hidden state \mathbf{S}_{i-1} .

$$\mathbf{q}_i, \mathbf{k}_j = \mathbf{W}_q \mathbf{x}_i, \mathbf{W}_k \mathbf{x}_j \in \mathbb{R}^{d_k} \quad (51)$$

$$\alpha_i = \sigma(\mathbf{W}_\alpha \mathbf{x}_i) \in \mathbb{R}^{d_k} \quad \beta_j = \sigma(\mathbf{W}_\beta \mathbf{x}_j) \in \mathbb{R}^{d_v} \quad (52)$$

$$\mathbf{v}_i = \mathbf{W}_v \mathbf{x}_i \in \mathbb{R}^{d_v} \quad (53)$$

$$\mathbf{S}_i = \alpha_i^\top \beta_i \odot \mathbf{S}_{i-1} + \mathbf{k}_i^\top \mathbf{v}_i \in \mathbb{R}^{d_k \times d_v} \quad (54)$$

$$\mathbf{z}_i = \mathbf{q}_i^\top \mathbf{S}_i \in \mathbb{R}^{d_v} \quad (55)$$

$$\mathbf{r}_i = \mathbf{W}_r \mathbf{x}_i \in \mathbb{R}^{d_v} \quad (56)$$

$$\mathbf{y}_i = \mathbf{W}_o(\text{swish}(\mathbf{r}_i) \odot \mathbf{z}_i) \in \mathbb{R}^d \quad (57)$$

Like linear attention and RetNet, GLA also has the following attention-style form.¹⁰

$$\mathbf{q}_i, \mathbf{k}_j = \mathbf{W}_q \mathbf{x}_i, \mathbf{W}_k \mathbf{x}_j \in \mathbb{R}^{d_k} \quad (58)$$

$$\alpha_i = \sigma(\mathbf{W}_\alpha \mathbf{x}_i) \in \mathbb{R}^{d_k} \quad \beta_j = \sigma(\mathbf{W}_\beta \mathbf{x}_j) \in \mathbb{R}^{d_v} \quad (59)$$

$$\mathbf{a}_i = \prod_j \alpha_{1:i} \in \mathbb{R}^{d_k} \quad \mathbf{b}_j = \prod_i \beta_{1:j} \in \mathbb{R}^{d_v} \quad (60)$$

$$\mathbf{v}_j = \mathbf{W}_v \mathbf{x}_j \in \mathbb{R}^{d_v} \quad (61)$$

$$\tilde{\mathbf{q}}_i = \mathbf{q}_i \odot \mathbf{a}_i \in \mathbb{R}^{d_k} \quad \tilde{\mathbf{k}}_j = \mathbf{k}_j / \mathbf{a}_j \in \mathbb{R}^{d_k} \quad \tilde{\mathbf{v}}_j = \mathbf{v}_j \odot \mathbf{b}_j \in \mathbb{R}^{d_v} \quad (62)$$

$$\mathbf{z}_i = \text{gla}(\mathbf{x}_{1:i}) = \left(\sum_{j=1}^i \mathbf{A}_{ij} \mathbf{v}_j \right) / \mathbf{b}_i \in \mathbb{R}^{d_v} \quad (63)$$

(rest is the same as the recurrent form)

\odot and $/$ denotes element-wise multiplication and division; σ denotes a sigmoid function.

Connections among Linear Attention, RetNet, GLA RetNet and GLA both inherit the basic linear recurrence with 2-D hidden states from linear attention. GLA and RetNet mainly differ in the decaying term from the perspective of the recurrent form. Specifically, GLA incorporates fine-grained data-dependent gates (α, β) whereas RetNet uses a single fixed decay λ that is shared across all tokens and hidden dimensions. The simplicity of decay in RetNet leads to neat attention-style form needed for parallel training. In comparison, GLA's attention-style form is more nuanced, thus resulting in a more complex training schema. Moreover, RetNet and GLA incorporate the additional output gate \mathbf{r}_i before the output projection \mathbf{W}_o . Such output gating is also used in LSTM and RWKV models presented below.

A.6 RWKV (Peng et al., 2023)

The recurrence of RWKV is motivated by attention-free network (Zhai et al., 2021), and it uses 1-D hidden state compared with the recurrences of linear attention.

$$\mathbf{k}_i = \mathbf{W}_k \mathbf{x}_i \in \mathbb{R}^{d_v} \quad \mathbf{v}_i = \mathbf{W}_v \mathbf{x}_i \in \mathbb{R}^{d_v} \quad (64)$$

$$\mathbf{a}_i = \exp(-\mathbf{w}) \odot \mathbf{a}_{i-1} + \exp(\mathbf{k}_i) \odot \mathbf{v}_i \in \mathbb{R}^{d_v} \quad (65)$$

$$\mathbf{b}_i = \exp(-\mathbf{w}) \odot \mathbf{b}_{i-1} + \exp(\mathbf{k}_i) \in \mathbb{R}^{d_v} \quad (66)$$

$$\mathbf{z}_i = \text{wkv}(\mathbf{x}_{1:i}) = \frac{\mathbf{a}_{i-1} + \exp(\mathbf{k}_i + \mathbf{u}) \odot \mathbf{v}_i}{\mathbf{b}_{i-1} + \exp(\mathbf{k}_i + \mathbf{u})} \in \mathbb{R}^{d_v} \quad (67)$$

$$\mathbf{r}_i = \mathbf{W}_r \mathbf{x}_i \in \mathbb{R}^{d_v} \quad (68)$$

$$\mathbf{y}_i = \mathbf{W}_o(\sigma(\mathbf{r}_i) \odot \mathbf{z}_i) \in \mathbb{R}^{d_v} \quad (69)$$

where $\mathbf{w}, \mathbf{u} \in \mathbb{R}^{d_v}$ are learnable parameters, σ is an activation function. The WKV operators maintain a recurrence with a pair of states $(\mathbf{a}_i, \mathbf{b}_i)$. Different from linear attention where the 2D hidden state is constructed via an outer-product $\mathbf{k}_i^\top \mathbf{v}_i$, WKV uses element-wise dot-product $\exp(\mathbf{k}_i) \odot \mathbf{v}_i$, thus the shape of the key and value vectors are the same.

¹⁰Please refer to the original paper for the derivation.

Since the decay term w is not data-dependent, WKV also has the following equivalent convolutional form:

$$\mathbf{k}_i = \mathbf{W}_k \mathbf{x}_i \in \mathbb{R}^{d_v} \quad \mathbf{v}_i = \mathbf{W}_v \mathbf{x}_i \in \mathbb{R}^{d_v} \quad (70)$$

$$\tilde{\mathbf{k}}\mathbf{v}_i = \exp(\mathbf{k}_i) \odot \mathbf{v}_i \in \mathbb{R}^{d_v} \quad \tilde{\mathbf{k}}_i = \exp(\mathbf{k}_i) \in \mathbb{R}^{d_v} \quad (71)$$

$$\mathbf{l}_i = \exp(-i\mathbf{w}) \in \mathbb{R}^{d_v} \quad (72)$$

$$\mathbf{a} = \mathbf{l} * \tilde{\mathbf{k}}\mathbf{v} \in \mathbb{R}^{L \times d_v} \quad (73)$$

$$\mathbf{b} = \mathbf{l} * \tilde{\mathbf{k}} \in \mathbb{R}^{L \times d_v} \quad (74)$$

(rest is the same as the recurrent form)

where $*$ denotes batched long convolution operator, i.e., one dimension of the filter $\mathbf{h}[:, i] \in \mathbb{R}^{L \times 1}$ handles one corresponding dimension $\mathbf{a}[:, i], \mathbf{b}[:, i] \in \mathbb{R}^{L \times 1}$.

A.7 S4 (Gu et al., 2022b)

Structured state space models (S4) is a family of sequence models defined with four parameters $(\Delta, \mathbf{A}, \mathbf{B}, \mathbf{C})$. S4 is typically represented as a sequence mapping of $\mathbb{R}^{L \times 1} \rightarrow \mathbb{R}^{L \times 1}$, wherein the input and output are both scalars (i.e. $\mathbf{x}, \mathbf{y} \in \mathbb{R}^1$). In this case, S4 has the following recurrent form.

$$\mathbf{h}_i = \bar{\mathbf{A}}\mathbf{h}_{i-1} + \bar{\mathbf{B}}\mathbf{x}_i \in \mathbb{R}^{d_k} \quad (75)$$

$$\mathbf{y}_i = \mathbf{C}\mathbf{h}_i \in \mathbb{R}^1 \quad (76)$$

where d_{inner} denotes the dimension of hidden states \mathbf{h}_i , $\bar{\mathbf{A}} \in \mathbb{R}^{d_{\text{inner}} \times d_{\text{inner}}}$ and $\bar{\mathbf{B}} \in \mathbb{R}^{d_{\text{inner}} \times 1}$ are transformed parameters for discrete sequence data according to a certain discretization rule (e.g., zero-order hold). $\mathbf{C} \in \mathbb{R}^{1 \times d_{\text{inner}}}$. Equivalently, it has the following convolutional form:

$$\bar{\mathbf{K}} = [\mathbf{C}\bar{\mathbf{B}}, \mathbf{C}\bar{\mathbf{A}}\bar{\mathbf{B}}, \dots, \mathbf{C}\bar{\mathbf{A}}^{L-1}\bar{\mathbf{B}}] \quad (77)$$

$$\mathbf{y} = \mathbf{x} * \bar{\mathbf{K}} \quad (78)$$

where $*$ denotes the convolution operator and $\bar{\mathbf{K}}$ denotes the convolution kernel. The convolution form is critical on enabling efficient parallel training via Fast Fourier Transform (FFT) algorithms.

Since the recurrent forms of other models are usually presented with vector input/output (i.e., $\mathbf{x}_i, \mathbf{y}_i \in \mathbb{R}^d$), we present its equivalent batched recurrent form as follows:

$$\mathbf{S}_i = \bar{\mathbf{A}} \circ \mathbf{S}_{i-1} + \bar{\mathbf{B}} \circ \mathbf{x}_i \in \mathbb{R}^{d \times d_{\text{inner}}} \quad (79)$$

$$\mathbf{y}_i = \mathbf{C} \circ \mathbf{S}_i \in \mathbb{R}^d \quad (80)$$

where \mathbf{S}_i denotes 2-D hidden states, $\bar{\mathbf{A}} \in \mathbb{R}^{d \times d_{\text{inner}} \times d_{\text{inner}}}$, $\bar{\mathbf{B}} \in \mathbb{R}^{d \times d_{\text{inner}} \times 1}$, $\mathbf{C} \in \mathbb{R}^{d \times 1 \times d_{\text{inner}}}$, \circ denotes batched matrix multiplication.¹¹ In this batched form, d numbers of independent SSM run in parallel, each responsible for a dimension of input \mathbf{x} .

Connections to Linear Attentions With this batched form in Equation (80), it becomes clear that S4, similar to linear attention, enjoys a large 2-D hidden states for recurrence. We can also draw a rough parallel between $(\bar{\mathbf{B}}, \mathbf{C})$ in S4 to $(\mathbf{q}_i, \mathbf{k}_j)$ in linear attention as they handle the input and output for the recurrences, respectively. The parallel reveals the difference between S4 and linear attention. In S4, the input and output mapping is not data-dependent, i.e., $(\bar{\mathbf{B}}, \mathbf{C})$ does not depend on input \mathbf{x} . In comparison, \mathbf{q}_i and \mathbf{k}_j are linear mappings of the input \mathbf{x}_i .

¹¹To differentiate the size of hidden states. in recurrences, we use \mathbf{h}_i in the 1-D cases; \mathbf{S}_i in the 2-D cases.

A.8 H3 (Dao et al., 2022)

H3 is a mixture of state-space models and linear attention. In particular, it employs the outer-product structure from linear attention (i.e., $\mathbf{k}_i^T \mathbf{v}_i$) to construct the input of a state-space model.

$$\mathbf{k}_i = \mathbf{W}_k \mathbf{x}_i \in \mathbb{R}^{d_k} \quad \mathbf{v}_i = \mathbf{W}_v \mathbf{x}_i \in \mathbb{R}^{d_v} \quad (81)$$

$$\mathbf{x}'_i = \mathbf{k}_i^T \mathbf{v}_i \in \mathbb{R}^{d_k \times d_v} \quad (82)$$

$$\mathbf{S}_i = \bar{\mathbf{A}} \odot \mathbf{S}_{i-1} + \bar{\mathbf{B}} \odot \mathbf{x}'_i \in \mathbb{R}^{d_k \times d_v \times d_{\text{inner}}} \quad (83)$$

$$\mathbf{z}'_i = \mathbf{C} \circ \mathbf{S}_i \in \mathbb{R}^{d_k \times d_v} \quad (84)$$

$$\mathbf{q}_i = \mathbf{W}_q \mathbf{x}_i \in \mathbb{R}^{d_k} \quad (85)$$

$$\mathbf{z}_i = \mathbf{q}_i \mathbf{z}'_i \in \mathbb{R}^{d_v} \quad (86)$$

$$\mathbf{y}_i = \mathbf{z}'_i \mathbf{W}_o \in \mathbb{R}^d \quad (87)$$

where $\bar{\mathbf{A}}, \bar{\mathbf{B}}, \mathbf{C} \in \mathbb{R}^{d_{\text{inner}}}$ are parameters of the state-space models, \odot denotes element-wise product with broadcasting, \circ denotes batched matrix-vector product. The SSM is diagonally parameterized (i.e., $\bar{\mathbf{A}}$ is a vector) and the original H3 paper additionally uses another shift-SSM (Dao et al., 2022) to further refine the key vector \mathbf{k}_i .

A.9 Hyena (Poli et al., 2023)

Hyena is a pure convolutional model that does not have an equivalent recurrent form, unlike S4. However, it recursively applies the convolution operator at the sequence level for N times (i.e., order- N Hyena). In practice, N is usually set to be 2, and the resulting form is as follows.

$$\mathbf{v}^n = \mathbf{W}_n \mathbf{x} \in \mathbb{R}^{L \times d} \quad (88)$$

$$\mathbf{z}^0 = \mathbf{v}^0 \in \mathbb{R}^{L \times d} \quad (89)$$

$$\left. \begin{aligned} \mathbf{l}_i^n &= \text{FFN}(i) \in \mathbb{R}^{L \times d} \\ \mathbf{z}^n &= \mathbf{v}^{n-1} \odot (\mathbf{l}^n * \mathbf{z}^{n-1}) \in \mathbb{R}^{L \times d} \end{aligned} \right\} \text{recursion } n = 1 \dots N \quad (90)$$

$$\mathbf{y} = \mathbf{z}^N \in \mathbb{R}^{L \times d} \quad (91)$$

where $*$ denotes batched convolution operator. In practice, the filter is padded to the size of $(2L - 1) \times d$ so that the convolution operator becomes a circular convolution for efficient training using FFT.¹² Note that the resulting kernels $\mathbf{l}^1, \mathbf{l}^2$ do not depend on input \mathbf{x} , but the convolution output is controlled by the data-dependent gate $\mathbf{v}^1, \mathbf{v}^2$ in Equation (90).

A.10 Mamba (Gu and Dao, 2023)

Mamba has the same recurrent form as S4, and uses data-dependent parameterization for $\bar{\mathbf{A}}, \bar{\mathbf{B}}, \mathbf{C}$:

$$\mathbf{v}_i = \mathbf{W}_v \mathbf{x}_i \in \mathbb{R}^{d_v} \quad (92)$$

$$\mathbf{S}_i = \bar{\mathbf{A}}_i \odot \mathbf{S}_{i-1} + \bar{\mathbf{B}}_i \odot \mathbf{v}_i \in \mathbb{R}^{d_k \times d_v} \quad (\odot \text{ with broadcast}) \quad (93)$$

$$\mathbf{y}_i = \mathbf{C}_i \mathbf{S}_i \in \mathbb{R}^{d_v} \quad (94)$$

where $\bar{\mathbf{A}}_i, \bar{\mathbf{B}}_i \in \mathbb{R}^{d_k \times d_v}$, $\mathbf{C}_i \in \mathbb{R}^{d_v}$ data-dependently parameterized, i.e., computed based on $\mathbf{x}_i / \mathbf{v}_i$. However, due to the data-dependence, this recurrent form no longer has an equivalent convolutional form for efficient training. The original paper handles this issue with customized hardware-efficient training algorithms based on the recurrent form.

B Optimization & Hyperparameter Search

We brute force search over grid of hyper-parameters in Table 2 and pick the best setting best on validation set on ICLL and AR separately. In AR we searched hidden sizes up to 256. In ICLL, we search first upto hidden size of 256, then if the best performing hidden size is 256, we try 512, and then 1024. We also used only best performing weight decay of 0.1 and learning rate of 2.5e-4 in the additional search runs.

¹²Please refer to Section 2 and 3 of (Poli et al., 2023) for details.

Hyper Parameter	Search
hidden size	[64, 128, 256, 512, 1024]
number of layers	[1, 2, 4, 8, 12]
number of heads	[1, 2, 4]
epochs	[200, 400]
batch size	32
optimizer	[AdamW]
└ learning rate	[1e-4, 2.5e-4]
└ weight decay	[0.01, 0.1]
└ β s	[(0.9, 0.99)]
scheduler	Cosine Scheduler with Warmup
└ minimum learning rate	2.5e-5
└ warm-up start learning rate	1e-7
└ warm-up steps	25000

Table 2: Hyper-parameter search space for neural models.

C Algorithms

C.1 In-context N-gram Language Model

Algorithm 1 In-context n-gram language model with back-off

- 1: **Input:** Current prefix of $s = x_{1:i-1}$ input, the n-gram order n
- 2: **Output:** Next token distribution
- 3: // Create in-context corpus from the prefix
- 4: $\mathcal{D} \leftarrow \text{map}(\text{add_padding_character}, \text{s.split}(\cdot))$
- 5: // Build all n-gram token counts up to order n
- 6: $c \leftarrow \text{count_all_n_grams}(\mathcal{D}; n)$
- 7: // Apply smoothing
- 8: $c^* \leftarrow \text{smoothing}(c)$
- 9: // To compute $P(x_i | x_{i-N+1}^{i-1})$ as :
- 10: **if** $c(x_{i-N+1}^i) > 0$ **then**
- 11: return $P(x_i | x_{i-N+1}^{i-1}) = \frac{c^*(x_{i-N+1}^i)}{c^*(x_{i-N+1}^{i-1})}$
- 12: **else**
- 13: Backoff to lower order model:
- 14: return $P(x_i | x_{i-N+1}^{i-1}) = \alpha(x_{i-N+1}^{i-1})P(x_i | x_{i-N+2}^{i-1})$
- 15: **end if**

In Algorithm 1, we present an **in-context** applied n-gram model that incorporates a back-off mechanism (Chen and Goodman, 1996). This model differs from the standard n-gram approach that is trained on the training set. Instead, here we train a unique n-gram for each example at each time step to predict the subsequent word. The back-off strategy allows for the assignment of non-zero probabilities to unseen n-grams by utilizing information from lower-order n-grams, as shown in line 14 of Algorithm 1. For each n-gram context x_{i-N+1}^{i-1} , the back-off weight $\beta(x_{i-N+1}^{i-1})$ can be computed as follows:

$$\beta(x_{i-N+1}^{i-1}) = 1 - \sum_{\{w | c(x_{i-N+1}^{i-1} w) > 0\}} \frac{c^*(x_{i-N+1}^{i-1} w)}{c^*(x_{i-N+1}^{i-1})} \tag{95}$$

In the absence of smoothing, the summation is expected to equal 1, resulting in β being 0. Smoothing techniques, such as laplace smoothing, modify the counts and allocate a probability mass for unseen n-grams. Alternatively, by excluding the probability corresponding to the padding token w , we can reserve probability mass for back-off without explicit smoothing. This approach is employed in our n-gram model implementation and it worked slightly better than add-one smoothing.

Finally, the back-off weights α calculated by normalizing beta for the lower-order n-gram probabilities for the unseen current n-gram sequences:

$$\alpha(x_{i-N+1}^{i-1}) = \frac{\beta(x_{i-N+1}^{i-1})}{\sum_{\{w|c(x_{i-N+1}^{i-1}w)=0\}} P(w | x_{i-N+2}^{i-1})} \quad (96)$$

It is important to note that the normalization ensures that the probabilities of all potential continuations of a given context sum to one.

C.2 In-context Baum-Welch HMM Language Model

Algorithm 2 In-context Baum-Welch HMM language model

Input: Current prefix of $s = \mathbf{x}_{1:i-1}$ input, number of states NS , a vocabulary \mathcal{V} , a maximum number of iterations N .
Output: Next token distribution
// Initialize the corpus from the prefix
 $O \leftarrow s.\text{split}(' \cdot')$
// Initialize the HMM parameters given the number of states and vocabulary
 $\lambda \leftarrow (A, B, \pi)$
for N times **do**
 // Expectation step (E-step)
 // Mask A to not have self transitions (see Appendix C.3)
 $A \leftarrow \text{mask_transitions}(A)$
 // Mask π to start at state 0 (see Appendix C.4)
 $\pi \leftarrow \text{mask_pi}(\pi)$
 $\xi, \gamma, b \leftarrow \mathbf{0}, \mathbf{0}, \mathbf{0}$
 for each observation sequence O^n **do**
 // Run forward-backward to get α and β
 $\alpha, \beta \leftarrow \text{forward-backward}(O^n | \lambda)$
 // Accumulate expected values for all time steps t , states l , next states m , tokens k
 $P(q_t = s_l | O^n, \lambda) \propto \alpha_t(l)\beta_t(l)$
 $P(q_t = s_l, q_{t+1} = s_m | O^n, \lambda) \propto \alpha_t(l)A_{lm}\beta_{t+1}(m)B_{mk}$
 // expected states
 $\gamma_t(l) \leftarrow \gamma_t(l) + P(q_t = s_l | O^n, \lambda)$
 // expected transitions
 $\xi_t(l, m) \leftarrow \xi_t(l, m) + P(q_t = s_l, q_{t+1} = s_m | O^n, \lambda)$
 // expected emissions
 $b(m, k) \leftarrow b(m, k) + 1_{O_t^i=k}P(q_t = s_m | O^n, \lambda)$
 end for
 // Maximization step (M-step)
 // Update state transition probabilities
 $A_{lm} \leftarrow \frac{\sum_{t=1}^{T-1} \xi_t(l, m)}{\sum_{t=1}^{T-1} \gamma_t(l)}$
 // Update emission probabilities
 $B_{mk} \leftarrow \frac{b_{mk}}{\sum_{t=1}^T \gamma_t(m)}$
 // Update initial state probabilities
 $\pi_l \leftarrow \gamma_1(l)/|O|$
 end for
 // Prediction Step
 // Run forward algorithm on the last observation to get α
 $\alpha \leftarrow \text{forward}(O^{\text{last}} | \lambda)$
 $p(x_i s) \propto \alpha_{|O^{\text{last}}|}(l)A_{lm}B_{mx_i}$
 return $p(x_i)$

Given a probabilistic automaton, PFA, from REGBENCH, we can construct a Hidden Markov Model (HMM) that assigns the same probabilities to any given string. The construction can be done as:

- For each pair of states $S_i, S_j \in \mathcal{S}$, create a corresponding HMM state $H_{(S_i, S_j)}$.
- Define the transition probabilities $A(H_{(S_i, S_j)}, H_{(S_l, S_m)}) \propto 1[j = l] \cdot T_{\text{PFA}}(S_i, w, S_j)$, where each character w transitions to a unique state in our PFAs.
- Set the emission probabilities $B(H_{(S_i, S_j)}, w) = 1$ if $T_{\text{PFA}}(S_i, w, S_j) > 0$, and 0 otherwise.
- Set initial state probabilities 1 for the start states and 0 for the others: $\pi(H_{(S_i, S_j)}) = 1[i == 1]$

The number of states in the constructed HMM is the square of the number of states in the probabilistic automaton. Therefore, we fit an HMM to the examples in REGBENCH with a maximum of $\text{NS} = 12^2 = 144$ states. Algorithm 2 details the in-context Baum-Welch predictor. We begin by constructing a list of observations from the current prefix $x_{1:i-1}$, and then fit an HMM given the global vocabulary \mathcal{V} and number of states $\text{NS} = 144$ using an improved Baum-Welch algorithm that is consistent with the structure of probabilistic automata in REGBENCH. We incorporate two pieces of prior information about the dataset:

C.3 Masking A to enforce state transitions

In our construction, we assume $A_{H_{(S_i, S_j)} H_{(S_l, S_m)}} = 0$ if $j \neq l$. We enforce this constraint in each iteration by masking the corresponding entries in A . Additionally, as our PFA sampling schema in Section 3.1 does not include self-transitions, we set all $A_{H_{(S_i, S_i)} H_{(S_i, S_i)}} = 0$.

C.4 Masking π to start at the initial state

All our PFAs have a single start state, which we denote as $H_{(S_0, S_i)}$ for all i , without loss of generality. We mask all other initial state probabilities such that $\pi(H_{(S_0, S_i)}) = 0$ for $i \neq 0$.

In our experiments, these masking strategies significantly improved the accuracy of the Baum-Welch algorithm. The results presented are based on this modified BW algorithm.

D Learned MLP Reweighting

We provide the training details of MLP n-gram reweighting models’ used in Section 5.3, namely LNW, LNW_r, and LNW_b.

Count Features (LNW Model) Given a data point $d = x_0 \dots x_i \dots x_l = x_0^l$, we first extract n-gram features for each position i and for each n-gram length n :

$$\text{gram}(i; n) = [\text{count}_{x_{1:i}}(x_{i-n}^{i-1} w) - 1 \quad \forall w \in \mathcal{V}] \in \mathcal{Z}^{|\mathcal{V}|} \tag{97}$$

The full set of n-gram features is the concatenation of n-gram features for $n = 1$ to $n = 3$:

$$\text{gram}(i; \leq 3) = \text{concatenate}(\text{gram}(i; 1), \text{gram}(i; 2), \text{gram}(i; 3)) \in \mathcal{Z}^{3|\mathcal{V}|} \tag{98}$$

We then train a sequence model that takes $\text{gram}(i; \leq 3)$ as input and applies a 2-layer MLP with GeLU activation to produce the unnormalized scores for the next token distribution. We use the same language modeling loss as in Equation (1). Our hyper-parameters for MLP training are as follows:

hyper parameter	value
hidden size	1024
epochs	50
batch size	32
optimizer	Adam
└ learning rate	1e-3
└ β_s	(0.9, 0.99)
scheduler	reduce on plateau
└ patience	5 epochs
└ factor	0.5
└ minimum learning rate	1e-5

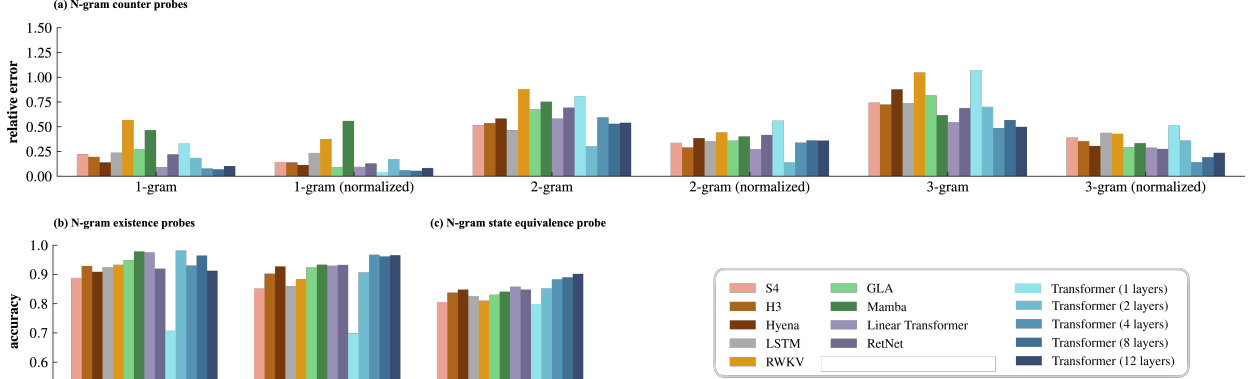


Figure 7: Additional results on probing analysis of n-gram representations with neural sequence models trained with $N_{\text{train}} = 40000$ examples. See Figure 5 for details.

Frequency Features (LNW_r Model) The frequency features model uses normalized n-gram features $\frac{\text{gram}(i;n)}{\sum \text{gram}(i;n)}$ instead of the raw n-gram features explained above.

Binary Features (LNW_b Model) The binary features model uses n-gram existence features, where $\text{n-gram}(i;n) = 1$ if the n-gram exists at position i and 0 otherwise, instead of raw n-gram features.

E Probing Experiments

Model and Objective We train a 2-layer Multilayer Perceptron (MLP) as our probe model in two configurations: **(1)** $f_{\text{n-gram}}(\mathbf{h}, \mathbf{c})$, where \mathbf{h} represents a hidden state at a specific time step and \mathbf{c} denotes the query n-gram; and **(2)** $f_{\text{equal}}(\mathbf{h}_i, \mathbf{h}_j)$, which is employed in state equivalence probes. The formulation of our $f_{\text{n-gram}}(\mathbf{h}, \mathbf{c})$ for an n-gram probe is as follows:

$$\mathbf{e}_c = W_{\text{embed}} \mathbf{c} \in \mathbb{R}^{n \times d/2} \quad (99)$$

$$\mathbf{e}_c = \text{flatten}(\mathbf{e}_c) \in \mathbb{R}^{nd/2} \quad (100)$$

$$\mathbf{e}_h = W_{\text{proj}} \mathbf{h} \in \mathbb{R}^{nd/2} \quad (101)$$

$$\mathbf{x} = \text{concatenate}([\mathbf{e}_c, \mathbf{e}_h, \mathbf{e}_c \odot \mathbf{e}_h]) \quad (102)$$

$$\mathbf{y} = W_2 \text{GeLU}(W_1 \mathbf{x} + b_1) + b_2 \quad (103)$$

where n is the order of the n-gram and d is the dimensionality of the hidden state used by the probe. For regression tasks, we employ the mean squared error loss on the output and our targets are corresponding n-gram counts or frequencies. While for classification tasks, we utilize binary cross-entropy loss with the logits being \mathbf{y} , and targets are whether the corresponding n-gram exists or not.

Data We train the probe using hidden states extracted from the actual training set of the models. Specifically, we randomly select an example from the training set, randomly choose a time step within that example, and then create a query n-gram by appending a random next character to the last $n - 1$ characters at the chosen time step. For regression tasks, we only consider n-grams that appear at least once in the prefix. Each epoch involves iterating over each example once. For testing, we apply the same sampling procedure using hidden states from the test set.

Model and Objective The state equivalence probe $f_{\text{equal}}(\mathbf{h}_i, \mathbf{h}_j)$ is defined as:

$$\mathbf{e}_i = W_{\text{proj}} \mathbf{h}_i \in \mathbb{R}^d \quad (104)$$

$$\mathbf{e}_j = W_{\text{proj}} \mathbf{h}_j \in \mathbb{R}^d \quad (105)$$

$$\mathbf{x} = \text{concatenate}([\mathbf{e}_i, \mathbf{e}_j, \mathbf{e}_i \odot \mathbf{e}_j]) \in \mathbb{R}^{3d} \quad (106)$$

$$\mathbf{y} = W_2 \text{GeLU}(W_1 \mathbf{x} + b_1) + b_2 \quad (107)$$

where d is the dimensionality of the hidden state used by the probe. We use the cross-entropy loss in the classification of whether two states are equivalent, and \mathbf{y} serves as the logits for cross-entropy.

Data Similar to the n-gram probe, we train the state equivalence probe using hidden states from the model’s training set. We randomly select an example and then sample two time steps within it, ensuring that in 50% of cases the probe receives identical states, and in the remaining 50%, it receives different states. The testing procedure mirrors that of the training phase.

We employ the following hyperparameters for all probe training. We train separate probes for each layer and present the best results in Figure 5 and Figure 7.

hyper parameter	value
hidden size (d)	128
epochs	1000
batch size	64
optimizer	Adam
└ learning rate	3e-4
└ β s	(0.9, 0.99)
scheduler	Cosine Annealing
└ minimum learning rate	1e-4

F N-gram Head

In Figure 8, we provide a Python implementation for n-gram layers that we use in our experiments.

```
def ngram_head(x, hidden_state, shift_step=1, ngram=1):
    """
    Args:
        x: bsz * input_len
        hidden_state: bsz * input_len * d_model
        ngram: 1 means bigram, 2 means trigram
        shift_step: which token to attend to after the matching ngram
    Output:
        bsz * input_len * d_model
    """
    bsz, seq_len = x.shape

    # bsz * L * L
    # match unigram as the first step
    mask_0 = x[:, None, :] == x[:, :, None]

    causal_mask = torch.tril(torch.ones(seq_len, seq_len,
                                         dtype=torch.bool, device=x.device), diagonal=-1)
    mask_0 = torch.logical_and(mask_0, causal_mask)

    masks = [mask_0.long()]
    for _ in range(1, ngram):
        # mask_0[i, j] = True means token i-1 and token j-1 is matched
        mask_0 = F.pad(mask_0, (1, -1, 1, -1), "constant", False)
        masks.append(mask_0.long())
    ngram_mask = torch.stack(masks, dim=-1).sum(dim=-1) >= ngram
    if shift_step > 0:
        ngram_mask = F.pad(ngram_mask,
                           (shift_step, -shift_step), "constant", False)
        ngram_mask = torch.logical_and(ngram_mask, causal_mask)

    # form a uniform distribution for matched tokens
    ngram_mask_norm = ngram_mask / ngram_mask.sum(dim=2, keepdim=True)
    ngram_mask_norm = torch.nan_to_num(ngram_mask_norm, 0)
    ngram_mask_norm = ngram_mask_norm.to(hidden_state.dtype)
    output = torch.einsum("bmn,bnz->bmz", ngram_mask_norm, hidden_state)
    return output
```

Figure 8: Python implementation of n-gram layers.

G Language model experiment

In the language model experiments, all models share the same following training hyperparameters. We plan to extend the experiment setting to larger models trained with more tokens in the future.

hyper parameter	value
hidden size (d)	1024
number of training tokens	7e9
number of warm-up tokens	5e8
batch size (number of tokens)	5e5
optimizer	AdamW
weight decay	0.01
└ learning rate	3e-4
└ β s	(0.9, 0.95)
scheduler	Cosine Annealing
└ minimum learning rate	3e-5